Accurate Prediction of Nonlinear Wave Forces : Part-I (Fixed Cylinder)

A.K. Swain S.A. Billings P.K. Stansby M. Baker

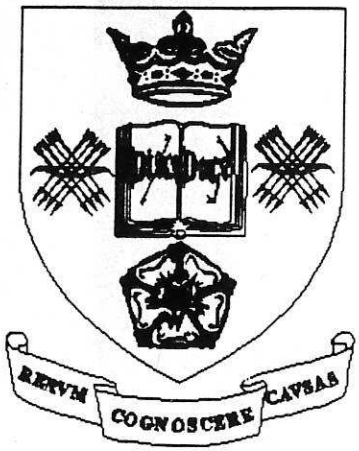

Department of Automatic Control and Systems Engineering
University of Sheffield, Post Box No:600,
Mappin Street, Sheffield, S1, 3JD (U.K)

Research Report No: 608
April, 1996

Accurate Prediction of Nonlinear Wave Forces : Part-I (Fixed Cylinder)

A.K.Swain ‡ S.A.Billings‡ P.K.Stansby† M.Baker*

‡ Department of Automatic Control and Systems Engineering
University of Sheffield, Po.Box-600, Mappin Street,S1,3JD,(U.K)

† Hydrodynamic Research Group,
School of Engineering, University of Manchester,
Manchester,M13,9PL,(U.K)

⋆ Department of Civil Engineering, University of Salford,
Salford,M7,1NU (U.K.)

Abstract

A new equation structure is proposed as an alternative to the Morison equation for the prediction of wave forces. Initially nonlinear parametric continuous time differential equation models were estimated from wave force data for a variety of flow situations by adopting a new approach which avoids direct differentiation of the input-output data. The method consists of two stages. The first stage involves estimation of a discrete time model (polynomial NARMAX) from sampled input-output data and computation of the linear and higher order frequency response functions. The second stage involves identifying continuous time models by curve fitting to the complex frequency response data using a weighted complex orthogonal estimator. The orthogonal property of the estimator helps in identifying the correct model structure or which terms to include in the model and the weighting property provides an additional degree of freedom to control the properties of the estimator with respect to the selection of the frequency range and number of data points. Morison equation models were initially fitted to the data but were shown to simply curve fit to the data without capturing the underlying dynamics. The frequency domain characteristics of the Morison equation models were also analysed and shown to be structurally deficient in representing certain dynamic features of the force. However, it is shown that the new equation structure is capable of emulating all

the relevant features of the wave force mechanics. The paper is organised into two parts. Part-I is concerned with the modelling of wave forces on a fixed cylinder and Part-II deals with a responding cylinder. Extensive simulations on a variety of experimental data show that models based on the new structure perform remarkably well compared with the Morison equation. For each flow situation, in addition to the drag and inertia coefficients of the Morison equation there are two non-dimensional coefficients defining history effects which show some consistency between widely different flow situations.

1 Introduction

An accurate and precise prediction of wave forces on offshore structures that are subjected to random ocean waves is an essential prerequisite for design. Wave forces on structures composed of slender members are traditionally calculated on the basis of the Morison equation which was introduced by Morison et al (1950) as a semi-intuitive expression predicting the force exerted on a body in a viscous fluid under unsteady flow conditions and is given by

$$\begin{aligned} F(t) &= \frac{1}{4}\pi\rho D^2 C_m \dot{u} + \frac{1}{2}\rho D C_d u|u| \\ &= K_i \dot{u} + K_d u|u| \end{aligned} \tag{1}$$

where 'F(t)' is force per unit axial length, 'u(t)' is the instantaneous flow velocity, 'ρ' is the water density and 'D' is the diameter,$K_i = \frac{1}{4}\pi\rho D^2 C_m$, $K_d = \frac{1}{2}\rho D C_d$. The dimensionless drag and inertia coefficients 'C_d' and 'C_m' depend on the characteristics of the flow. More recently the general validity of Morison's equation and particularly the validity in relation to wave induced loads on circular cylinders has been questioned. Specifically the determination of C_d and C_m at high Reynolds numbers has presented a formidable problem that has endured for many years. Although much progress in the basic understanding of oscillatory flow has been made, many uncertainties and conditions in the reported data and conclusions still exist (Sarpkaya and Issacsson,1981, Chakrabarti,1987). The Morison equation generally predicts the main trends in measured data quite well; however some characteristics of the flow are not well represented. For example i n sinusoidal oscillatory flow the force variation at the fundamental frequency may be well predicted while that at higher harmonics is not. This implies that peak forces may be poorly predicted. A poor representation of the high frequency content of the forces is a serious limitation for the determination of the fatigue life of a structural element. Hence Morison's equation needs to be extended.

An attempt to determine new model structures to predict the wave forces has been made by Stansby et al(1992). These authors showed that two simple extended equations allowed a considerable increase in the accuracy of curve fits to data measured in a variety of flow situa-

tions. A sophisticated system identification technique based on the Nonlinear Auto Regressive Moving Average with eXogenous inputs (NARMAX)(Leontraritis and Billings,1985) model was used by Worden et al (1994) to model the wave force dynamics of U-tube,De-Voorst and Christchurch Bay data. Although the discrete NARMAX models obtained could adequately represent the dynamics of the input-output data and performed well compared to the Morison equation so far as the predictive performance was concerned, the parameters of the discrete models could not be easily related to the physical parameters of the inherently continuous time system. Hence, it is often desirable to fit continuous time models to the input-output data to obtain physically interpre table parameters.

Identification of continuous time models from input-output data has been studied by several authors in the past and comprehensively documented by Unbehauen and Rao(1987). Most of the techniques developed so far are limited to the identification of linear systems and make use of several types of modulating function,state variable filters,Poison filter chains and chain integrators in order to avoid direct differentiation of the process data. Extending these techniques to the identification of nonlinear systems is much more involved.

An alternative indirect approach is to estimate the parameters of a continuous time differential equation model by curve fitting to the system frequency response functions. But when the system is nonlinear,computation of the higher order frequency response functions directly from input-output data involves extending the classical cross and power spectral density concepts to multidimentions and using correlation or FFT based techniques coupled with multidimensional windowing and smoothing (Kim and Powers,1988). An indirect approach is to estimate a linear or nonlinear discrete time model from sampled input-output data and then to compute the higher order frequency response functions from the unbiased process model using the recursive algorithm proposed in Billings and Tsang(1989),Peyton Jones and Billings,1989). The latter approach offers significant advantages since only small data sets are required and the complexities of multi dimensional windowing and smoothing are avoided.

The present study attempts to find continuous time models which accurately represent the nonlinear wave force data by parameterising the system frequency response functions in terms of the coefficients of a nonlinear ordinary differential equation (Tsang and Billings,1992, Swain and Billings,1995). The motivation for this approach comes from the fact that the discrete representation of a continuous time system is not unique. Thus different discrete time models can be obtained for the same system. But whatever models are obtained,if the models have captured the dynamics of the system adequately, the frequency response functions must be the same. The present method therefore utilizes the invariant information in the frequency response functions to fit continuous time models. The procedure consists of three steps

- Identify a discrete time model (polynomial NARMAX) using sampled input-output data

- Compute the linear and nonlinear frequency response functions using the algorithms of Tsang and Billings (1989), Peyton Jones and Billings (1989).
- Identify the continuous time models by curve fitting to the frequency response functions using the weighted complex orthogonal estimator (Swain and Billings,1995).

Based on the observations of the experimental data and from preliminary mathematical analysis of the Morison equation, a new equation structure is proposed for prediction of wave forces.

The organisation of the paper proceeds as follows. Section-2 highlights the preliminary characteristics of the Morison equation. A brief tutorial concerning the concepts and techniques of fitting discrete parametric models (NARMAX) from sampled input-output data is presented in section 3. The concept of frequency domain analysis and the interpretation of generalised frequency response functions (GFRF) are briefly introduced in section-4. The procedure of identifying nonlinear continuous time differential equation models from complex frequency response data using the weighted complex orthogonal estimator is described in section-5. Identification of nonlinear differential equation models from several data sets is carried out in section-6-8. Section-9 further analyses the behavior of the Morison equation from the point of view of system identification and a new equation structure is proposed for the prediction of wave forces. Continuous time models are fitted based on the proposed structure using least squares

and the results show that the estimated nonlinear continuous time models are capable of emulating all the dynamic features of the wave force data and are a significant improvement compared to the Morison equation.

2 Frequency Domain Characteristics of Morison's Equation

Since the final objective of the present study is to fit nonlinear continuous time models of the wave forces,it will be appropriate to begin by analysing the general behavior of the Morison equation. A comparative analysis of the Morison model and the discrete NARMAX model for specific sets of data has been made in the practical examples.

It is not possible to directly map the Morison equation into the frequency domain using the techniques of Volterra series due to the presence of the drag term $u|u|$ which has a discontinuous second derivative, since a necessary condition for the existence of the Volterra series is that all nonlinearities must be infinitely differentiable (Palm and Poggio,1977). However it

is possible to approximate the drag term $u|u|$ in eqn(1) as a polynomial of the form

$$u|u| = a_1 u + a_2 u^2 + a_3 u^3 + a_4 u^4 + a_5 u^5 + ... \tag{2}$$

Under the assumption that the input signal is a zero mean Gaussian signal whose odd order moments are identically zero (often a reasonable assumption), eqn(2) can be represented as an odd order polynomial of the form

$$u|u| = a_1 u + a_3 u^3 + a_5 u^5 + ... \tag{3}$$

The approximated Morison equation is therefore given by

$$\begin{aligned} F(t) &= K_i \dot{u} + K_d(a_1 u + a_3 u^3 + a_5 u^5 + ...) \\ &= K_i \dot{u} + K_{d1} u + K_{d3} u^3 + K_{d5} u^5 + ... \end{aligned} \tag{4}$$

where $K_{d1} = K_d a_1$, $K_{d3} = K_d a_3$ and so on. The analysis of the approximated Morison equation is possible using techniques of the Volterra series. Assuming that the drag term can be approximated with reasonable accuracy by a third order polynomial of the input, the approximated Morison equation is given by

$$F(t) = K_i \dot{u} + K_{d1} u + K_{d3} u^3 \tag{5}$$

The linear and third order transfer function of the approximated Morison equation of eqn.(5) are given by

$$H_1(j\omega_1) = K_{d1} + j\omega_1 K_i \tag{6}$$

$$H_3(j\omega_1, j\omega_2, j\omega_3) = K_{d3} \tag{7}$$

From the linear transfer function eqn.(6) it is obvious that as $\omega_1 \rightarrow \infty$, the magnitude $|H_1(j\omega_1)| \rightarrow \infty$ which means that when the cylinder is subjected to a high frequency input wave of very small amplitude, it will experience an extremely high force. The third order frequency response function is a constant independent of the frequency of the input wave.

The intrinsic characteristic of the Morison equation is such (as evident from its linear transfer function) that it can adequately capture the dynamics of a system whose linear gain increases with the frequency of the input signal. But often in the case of most practical systems, the gain of the system falls off as the frequency increases. It will be obvious in the examples when models are fitted to the real data that Morison's equation may require modification and extension.

The first step in the search for a possible extension of the Morison equation is to fit

continuous time models to the input-output (velocity-inline force) data for a variety of flow situations and look for any consistency in the models. However, estimation of continuous time differential equation models from raw input-output data involves differentiation of the data and hence may result in incorrect parameter estimates due to the presence of noise inherent in practical data. To avoid errors due to differentiation, a new approach is followed in the estimation process where a discrete NARMAX model is initially fitted to the data and then continuous time models are fitted to the frequency response functions which are computed from the NARMAX model. Note that one of the most important advantages of the NARMAX model is that the process terms and noise terms are decoupled from each other;thus the computed frequency response functions from the process model are noise free.

Prior to the estimation of continuous time models; the relevant theoretical prerequisites of the procedure adopted in the estimation phase are briefly presented in tutorial form in section-3-5.

3 System Identification in the Discrete Domain-the Polynomial NARMAX Model

The problem of system identification is primarily concerned with the mathematical representation of a linear or nonlinear input output relationship. The mathematical model representation basically depends on the identification methods considered and the structure of the data that are available. The identification of nonlinear systems using the functional series expansion of Volterra and related methods have been well documented in a comprehensive way by Billings(1980). The representation of a nonlinear system by the functional series expansion of Volterra or Wiener that maps past inputs into the present outputs, requires an excessive parameter set often extending to well in excess of 500 kernel values even for simple nonlinear systems and hence proves to be impractical.

However,the difficulty of excessive parameters associated with the Volterra modelling of nonlinear systems can be overcome by representing the system by a discrete parametric model. One of the possible choices is the NARMAX model (Nonlinear Auto Regressive Moving Average with eXogenous inputs); initially proposed by Billings and Leonataritis(1982). It has been proved by Leontaritis and Billings (1985),that a nonlinear discrete-time time invariant system can always be represented by the NARMAX model

$$y(k) = F^{N_l}[y(k-1),...y(k-n_y),u(k-1),...u(k-n_u),e(k-1),...e(k-n_e)] + e(k) \quad (8)$$

in a region around an equilibrium point provided the response function of the system is finitely realizable and a linearised model would exist if the system were to be operated close

to the chosen equilibrium point, where y(k),u(k) and e(k) represent the output, input and noise respectively at time intervals 'k'. n_y,n_u,n_e are the corresponding lags and $F^{N_l}[.]$ is some nonlinear function. In practice the noise e(k) can not usually be measured and is replaced by the prediction errors defined as

$$\epsilon(k) = y(k) - \hat{y}(k) \tag{9}$$

where $\hat{y}(k)$ is the one step ahead prediction of y(k).

It should be noted that the model includes both linear and nonlinear noise components. If the system is nonlinear any noise that arises is also likely to enter in a nonlinear manner. Although all these terms correspond to unmeasurable states,they must be included in the model, otherwise the estimated parameters will contain systematic errors called bias.

3.1 Structure Detection and Parameter Estimation

In the present study the map $F^{N_l}[.]$ is taken to be a polynomial of degree 'N_l' but $F^{N_l}[.]$ can be defined as a neural network, rational function expansion etc. In order to estimate the parameters of this map, eqn(8) is expressed in prediction error form as

$$y(k) = \sum_{i=1}^{N_t} \theta_i x_i(k) + e(k) \tag{10}$$

where N_t is maximum number of terms in the NARMAX model and is given by

$$\begin{aligned} N_t &= \sum_{i=0}^{N_l} n_i \qquad n_0 = 1 \\ n_i &= n_{i-1}(n_y + n_u + n_e + i - 1)/i, \qquad i = 1, ...N_l \end{aligned} \tag{11}$$

and

$$\begin{aligned} x_1(k) &= 1 \\ x_i(k) &= \prod_{j=1}^{p_y} y(k - n_{y_j}) \prod_{k=1}^{q_u} u(k - n_{u_k}) \prod_{m=1}^{r_e} e(k - n_{e_m}) \end{aligned} \tag{12}$$

$i = 2, ...n, \qquad p_y, , q_u, r_e \geq 0 \; ; \qquad 1 \leq p_y + q_u + r_e \leq N_l;$

$1 \leq n_{y_j} \leq n_y, \qquad 1 \leq n_{u_k} \leq n_u, \qquad 1 \leq n_{e_m} \leq n_e$ and 'N_l' is the degree of polynomial expansion.

By convention $p_y = 0$ indicates that $x_i(k)$ contains no $y(.)$ terms. Similarly $q_u = 0$ indicates that $x_i(k)$ contains no $u(.)$ terms and $r_e = 0$ indicates that $x_i(k)$ contains no e(.)

terms. Regrouping terms in eqn(8) yields

$$y(k) = F^p[y(k-1),..y(k-n_y),u(k-1)...u(k-n_u)]$$
$$+F^n[y(k-1)...y(k-n_y),u(k-1),...u(k-n_u),e(k-1),...e(k-n_e)]+e(k) \quad (13)$$

where $F^p[.]$ contains all terms $\theta_i x_i(k)$ with $r_e = 0$ and $F^n[.]$ contains all terms $\theta_i x_i(k)$ with $r_e \neq 0$. $F^p[.]$ is referred to as the process model and $F^n[.]$ as the noise model. When the system is nonlinear direct estimation based on eqn.(13) may involve an excessive number of terms. Simply increasing the orders n_y,n_u and n_e and the degree 'N_l' of the polynomial expansion to achieve the desired accuracy will in general result in an excessively complex model and possibly numerical ill-conditioning. The determination of the structure or which terms to include in the model is therefore essential if a parsimonious model is to be determined from the large number of candidate terms(eqn.(11)). An orthogonal regression estimator Billings et al(1988) can select a subset of significant terms very efficiently. The basic idea is to transfer the model of eqn.(13) into an equivalent orthogonal equation. Because of the orthogonal property,signif icant terms can be determined in a particularly simple forward regression procedure. The criterion for selecting terms is based upon the proportion of the output variance that each term contributes.

An advantage of the orthogonal estimator is that significant parameters can be determined recursively and quite independently of the other terms already selected. Furthermore,the estimation of the process and noise model parameters can be decoupled. This is particularly useful for the identification of the model of eqn.(13). A parsimonious process model is first determined. This model will not be affected by whatever noise model is produced later. The initial prediction errors are computed based on this process model and a noise model can then be selected. A revised prediction error sequence is then calculated and an improved noise model is determined.

3.2 Model Validity Tests

After fitting a NARMAX model to the input-output data, it is important to test for possible inadequacies of the fitted model, that is to check if the model has successfully captured the system dynamics and is not just a curve fit to one data set. The problems of curve fitting are discussed in the examples. Over the last few years a lot of work has been reported in the system identification literature relating to the design and development of model validation tools by Billings and co-workers (Billings and Voon,1986,Billings and Zhu,1994). In the present study, the models are validated based on the predictive performance (cross validation) and correlation tests.

3.2.1 Cross Validation

One technique which can be used to judge the qualitative performance of a model is to assess the predictive performance based on both one-step ahead prediction of the system output defined as

$$\hat{y}_{osa}(k) = F^{N_l}[y(k-1),\ldots,y(k-n_y),u(k-1),\ldots,u(k-n_u),e(k-1),\ldots e(k-n_e)] \quad (14)$$

and the model predicted output given by

$$\hat{y}_{mpo}(k) = F^{N_l}[\hat{y}_{mpo}(k-1),\ldots,\hat{y}_{mpo}(k-n_y),u(k-1),\ldots,u(k-n_u)] \quad (15)$$

A metric which measures the closeness of fit between the predicted output and measured output is the normalised root mean square error(NMSE) which is defined as (Weigend and Gershenfeld,1993)

$$NMSE = \sqrt{\frac{\sum(\hat{y}(k)-y(k))^2}{\sum(y(k)-\overline{y})^2}} \quad (16)$$

where $\hat{y}(k)$ is the predicted (either one-step ahead or model predicted) output of the system. Another approach commonly known as cross validation, is based on dividing the available data set into two disjoint sets, the estimated and the test set. The former is used for estimation and the latter set is used for model validation.

3.2.2 Correlation Tests

The classical approach to validating identified linear models consists of computing the auto-correlation function of the residuals and the cross-correlation function between the residuals and the input(Soderstrom and Stoica,1989). This result has been extended by Billings and co-workers to the case of validating identified nonlinear models (Billings and Voon,1986, Billings and Zhu,1994). The identified model will only produce acceptable predictions over different data sets if it is unbiased. If the model structure and the estimated parameters are correct then the prediction error sequence $\epsilon(k)$ should be unpredictable from all linear and nonlinear combinations of past inputs and outputs. This condition will hold if and only if the following conditions hold

$$\begin{aligned}
\phi_{\epsilon\epsilon}(\tau) &= E[(\epsilon(k-\tau)\epsilon(t)] &&= \delta(\tau), \\
\phi_{u\epsilon}(\tau) &= E[u(k-\tau)\epsilon(t)] &&= 0, \quad \forall\,\tau, \\
\phi_{[uu]^n\epsilon}(\tau) &= E[(u^2(k-\tau)-\overline{u^2(t)})\epsilon(t)] &&= 0, \quad \forall\,\tau, \\
\phi_{[uu]^n\epsilon^2}(\tau) &= E[(u^2(k-\tau)-\overline{u^2(t)})\epsilon^2(t)] &&= 0, \quad \forall\,\tau, \\
\phi_{(\epsilon)[\epsilon u]}(\tau) &= E[\epsilon(t)\epsilon(k-1-\tau)u(k-1-\tau)] &&= 0, \quad \tau \geq 0.
\end{aligned} \quad (17)$$

where $\delta(\tau)$ is the *Kronecker delta*. The over-bar signifies mean value and $E[.]$ denotes expectation. The underlying rationale of the correlation tests is that for a model to be statistically valid, there should be no predictable information in the residuals. However, in practice only a finite data length will be available which is contaminated with noise (which is rarely additive, Gaussian or white) measured with finite precision and subject to innumerable external influences in the environment and the measurement apparatus. Hence confidence bands should be used to indicate if the correlation between variables is significant or not. For large N, the 95% confidence bands are approximately $\pm \frac{1.96}{\sqrt{N}}$ and any significant correlation will be indicated by points lying outside the respective confidence band.

3.3 Preprocessing of the Data

Before estimation, the raw data may require preprocessing e.g. removal of any possible trends in the data and suitable choice of sampling time, in order to avoid possible numerical ill-conditioning and identifiability problems.

3.3.1 Choice of Sampling Time

A judicious choice of sampling time is central to the success of any identification algorithm. A lot of studies have been made by several authors in the past (Iserman,1980,Ljung,1987) for selecting proper sampling times for identifying and controlling linear systems. The sampling time should neither be too small nor too large. Too small a sampling time causes the data vector to be autocorrelated and hence involves singularity of the information matrix. Too large a sampling time can cause a loss of information i.e. the inter sample behavior contains a lot of information. All the observations by the authors in the past are based on a rule of thumb. These suggest that for successful control and identification of a linear system,the sampling time T_s should lie between $\frac{1}{10}$th to the $\frac{1}{20}$th of the dominant time constant of the system or at least 15 to 20 samples should be taken between 95% of the settling time of the system.

The choice of sampling times for nonlinear systems has received relatively little attention in the past until recently when Billings and Aguirre(1994) showed that the sampling time which enhances model structure selection is not necessarily the best choice of sampling time for parameter estimation and vice versa. Billings and Aguirre (1994) suggested several rules for selecting the sampling time but the most practical and easiest method is to analyse the linear and nonlinear correlation functions of the output. Consider the correlation functions

$$\begin{aligned} \phi_{yy}(\tau_c) &= E[(y(k)-\overline{y(k)})(y(k-\tau_c)-\overline{y(k)})] \\ \phi_{y^2y^2}(\tau_c) &= E[(y^2(k)-\overline{y^2(k)})(y^2(k-\tau_c)-\overline{y^2(k)})], \tau_c = 0,1,..... \end{aligned} \tag{18}$$

Then determine

$$\tau_m = min[\tau_y, \tau_{y'^2}] \tag{19}$$

where τ_y is the time of the first minimum of $\phi_{yy}(\tau)$ and $\tau_{y'^2}$ is defined analogously. Finally the sampling time can be chosen as follows. $\frac{\tau_m}{20} \leq T_s \leq \frac{\tau_m}{10}$

It should be emphasised here that the above procedure only provides a guide to the selection of sampling time. The choice differs from process to process and upon the requirements of the analyst.

4 Frequency Domain Analysis and Interpretation

In the last section, procedures for fitting discrete NARMAX models were discussed. However, the discrete polynomial NARMAX representation of a particular system is not necessarily unique which means that it is possible to get different discrete models for the same system; thus one can not be sure if the difference in model structure is due to differences in the underlying physics or if it is simply a reflection of non-uniqueness. However, no matter what the form of the model, if the model correctly captures the dynamics associated with the data sufficiently, this must reflect the correct linear and nonlinear frequency content of the system. In other words, although there may be a number of discrete time models that represent a continuous time system, the higher order frequency response functions corresponding to each of the discrete models should correspond with those for the continuous time system description. This forms the motivation for analysing the above systems in the frequency domain.

Since continuous time differential equation models are to be estimated for different sets of wave force data by curve fitting to the generalised frequency response functions which are computed by mapping the NARMAX models into the frequency domain, a brief review of this will be given below.

The n-th order generalised frequency response function (GFRF) of a system is defined as

$$H_n(j\omega_1, ...j\omega_n) = \int_{-\infty}^{\infty} ... \int_{-\infty}^{\infty} h_n(\tau_1, ..., \tau_n) exp(-j(\omega_1\tau_1 + ...\omega_n\tau_n))d\tau_1....d\tau_n \tag{20}$$

where $h_n(\tau_1, ...\tau_n)$ is known as the 'nth' order Volterra Kernel or generalised impulse response function of order 'n' . The frequency domain representation of a system having nonlinearity of degree 'N_l' is given as

$$\begin{aligned} Y(j\omega) &= \sum_{n=1}^{N_l} Y_n(j\omega) \\ &= \sum_{n=1}^{N_l} \frac{1}{2\pi^{n-1}} \int_{-\infty}^{\infty} ... \int_{-\infty}^{\infty} H_n(j\omega_1, ...j\omega_n) U(j\omega_1)...U(j\omega_n) \end{aligned} \tag{21}$$

where $\omega = \omega_1 + \omega_2 + ... + \omega_n$, $Y(j\omega)$ and $U(j\omega)$ represent spectrum of output and input respectively.

For example, if a system were represented by a Volterra series of order three, then

$$Y(j\omega) = H_1(j\omega_1)U(j\omega_1) + \frac{1}{2\pi}\int_{-\infty}^{\infty} H_2(j\omega_1, j\omega_2)U(j\omega_1)U(j\omega_2)d\omega_1 + \frac{1}{(2\pi)^2}\int_{-\infty}^{\infty}\int_{-\infty}^{\infty} H_3(j\omega_1, j\omega_2, j\omega_3)U(j\omega_1)U(j\omega_2)U(j\omega_3)d\omega_1 d\omega_2 \quad (22)$$

4.1 Relevant Frequencies of the GFRF Plots

An important property of nonlinear systems is that new frequencies may be generated in the output including harmonics and intermodulation effects caused by the nonlinear interaction and mixing of input frequency components. These phenomena are captured by the generalised frequency response functions.

If a system possessing an n-th order nonlinear term is excited by an input signal that is strictly band limited such that it has no spectral components above some frequency $(\omega_u)_{max}$, the maximum frequency $(\omega_y)_{max}$ of the output will contain n-th order harmonics of the highest frequency of the input and will thus satisfy the relation

$$(\omega_y)_{max} = n(\omega_u)_{max} \quad (23)$$

The sampling frequency 'ω_s' must therefore satisfy the following inequalities to avoid aliasing

$$\begin{aligned} \omega_s &\geq 2 \times (\omega_y)_{max} \\ &\geq 2 \times n(\omega_u)_{max} \end{aligned} \quad (24)$$

Furthermore, the 'nth' order GFRF $H_n(j\omega_1, ...j\omega_n)$, which is a multidimensional function will generate an intermodulation frequency $\omega = \omega_1 + ..\omega_n$ in the output for a particular combination $(\omega_1, ...\omega_n)$ in the input frequency space. Since input-output signals are sampled at the sampling frequency ω_s, only those frequencies within the fundamental range $[\frac{-\omega_s}{2}, \frac{\omega_s}{2}]$ are meaningful. Hence it is required that $\omega = \omega_1 + ...\omega_n$ should be kept within the fundamental frequency range. Since each frequency variable $\omega_1, ...\omega_n$ in the n-tone input varies independently, the relevant range for the n-th order frequency response function $H_n(j\omega_1, ..j\omega_n)$ is $\omega_i \leq \frac{\omega_s}{2n}$. The value of the generalised frequency response functions beyond this frequency range should therefore be ignored.

4.2 Interpretation of Generalised Frequency Response Functions

The generalised frequency response functions of discrete NARMAX models can be obtained using the recursive algorithm of Peyton Jones and Billings (1989). The frequency at which the magnitude of the linear transfer function $H_1(j\omega_1)$ is maximum is the linear resonant frequency of the system (say ω_r). This indicates that for this frequency of excitation, the amplitude of the linear part of the response $y_1(t)$ is a maximum. Similarly it is possible to interpret the higher order frequency response functions from the magnitude and contour plots. For example, the ridges in the contour plot of the higher order frequency response functions are equivalent to the peaks in the linear frequency response plot $H_1(j\omega_1)$. Thus if the equation of the ridge in the n-th order transfer function is given by $\omega_1 + \omega_2 + ...\omega_n = \omega_{nlr}$, this indicates that the n-th order output $y_n(t)$ of the system will be a maximum if the system is excited by an input whose frequency sum equals ω_{nlr}.

To further improve the understanding and interpretation of the generalised frequency response plots, consider as an example a system which is modelled by the NARMAX model of the form

$$y(k) = a_1 y(k-1) + a_2(y(k-2) + b_1 u(k-1) + b_2 u(k-2) + c_1 u(k-1)u(k-2)u(k-3) \quad (25)$$

The linear transfer function of this system is given by

$$\begin{aligned} H_1(j\omega_1) &= (b_1 e^{-j\omega_1} + b_2 e^{-j2\omega_1}).\frac{1.0}{1 - a_1 e^{j\omega_1} - a_2 e^{-j2\omega_1}} \\ &= H_1^{(MA)}(j\omega_1).H_1^{(AR)}(j\omega_1) \end{aligned} \quad (26)$$

where $H_1^{(MA)}(j\omega_1)$ corresponds to the part of the linear transfer function due to pure input terms only (Moving Average part) and $H_1^{(AR)}(j\omega_1)$ corresponds to the part of $H_1(j\omega_1)$ due to pure linear output terms (Auto Regressive part).

Since the model does not posses any second order nonlinear terms, the second order transfer function $H_2(j\omega_1, j\omega_2)$ is absent. The analytical expression for the third order frequency response function of the system is given by

$$H_3(j\omega, j\omega_2, j\omega_3) = \frac{c_1 e^{-j(\omega_1+2\omega_2+3\omega_3)}}{1 - a_1 e^{-j(\omega_1+\omega_2+\omega_3)} - a_2 e^{-j2(\omega_1+\omega_2+\omega_3)}} \quad (27)$$

Note that for the present case, the contribution of the nonlinear term to the magnitude of $H_3(.)$ is c_1 since the magnitude of the phasor remaining in the numerator of $H_3(.)$ is unity. Comparing the expression for $H_3(.)$ with that of $H_1^{(AR)}(.)$ in eqn(26), it will be obvious that if ω_r^{AR} is the resonant frequency of $H_1^{(AR)}(.)$, the maximum in the magnitude of $H_3(.)$ will occur when $\omega_1 + \omega_2 + \omega_3 = \omega_r^{AR}$. Thus if a system possesses pure input nonlinearity, the peak

in the magnitude of $H_3(.)$ will occur at those combinations of input frequencies whose sum equals the resonant frequency of the autoregressive part of the linear transfer function.

5 Reconstruction of Nonlinear Continuous Time Models

Before a nonlinear continuous time model can be fitted to the frequency response data the form of the general nonlinear continuous time model must be defined. Consider a system whose dynamics are described by the nonlinear differential equation

$$\sum_{m=1}^{N_l}\sum_{p=0}^{m}\sum_{l_1,l_{p+q}=0}^{L} c_{p,q}(l_1,..l_{p+q})\prod_{i=1}^{p} D^{l_i}y(t)\prod_{i=p}^{p+q} D^{l_i}u(t) = 0 \tag{28}$$

where 'L' is the maximum order of the differential; N_l is the maximum degree of nonlinearity, $p+q=m$, and $m=1,....N_l$ corresponds to various orders of nonlinearity. The operator 'D'is the differential operator. Once 'm' takes a specific number,all the mth-order terms, each of which contains a pth-order factor in '$D^{l_i}y(t)$' and a qth-order factor in '$D^{l_i}u(t)$', subject to $p+q=m$, are included and each term is multiplied by a coefficient $c_{p,q}(l_1,...l_{p+q})$ while the multiple summation over the $l_i(l_i=0...L)$ generates all possible permutations of differentiations. For example, the general linear differential equation is included in the above form by setting the order of nonlinearity 'm' as 1 to give:

$$\sum_{l_1=0}^{L} c_{1,0}(l_1)D^{l_1}y(t) + \sum_{l_1=0}^{L} c_{0,1}(l_1)D^{l_1}u(t) = 0. \tag{29}$$

As an example the differential equation

$$\frac{d^2y}{dt^2} + 2.5\frac{dy}{dt} + 1.0y + 1.2\frac{du}{dt} + u + 100y^2 + 50u^2 + 10^4y^3 + 25.0(\frac{dy}{dt})u^2 = 0 \tag{30}$$

would be represented by the model of eqn.(28) with following definitions
$c_{1,0}(0)=1.0$, $c_{1,0}(1)=2.5$, $c_{1,0}(2)=1.0$, $c_{0,1}(0)=1.0$, $c_{0,1}(1)=1.2$, $c_{2,0}(0,0)=100.0$, $c_{0,2}(0,0)=50.0$, $c_{3,0}(0,0,0)=10^4$, $c_{1,2}(1,0,0)=25.0$

The frequency domain equivalent of eqn(28) is based on the generalised frequency response functions which are given by mapping the time-domain representation into the frequency domain (Billings and Peyton-Jones,1990)

$$-\left[\sum_{l_1=0}^{L} c_{1,0}(l_1)(j\omega_1+....j\omega_n)^{l_1}\right] H_n^{asym}(j\omega_1,...j\omega_n)$$

$$= \sum_{l_1,l_n=0}^{L} c_{0,n}(l_1,...l_n)(j\omega_1)^{l_1}.....(j\omega_n)^{l_n}$$

$$+\sum_{q=1}^{n-1}\sum_{p=1}^{n-q}\sum_{l_1,l_n=0}^{L} c_{p,q}(l_1,...l_{p+q})(j\omega_{n-q+1})^{l_{p+1}}...(j\omega_n)^{l_{p+q}}H_{n-q,p}(j\omega_1,..j\omega_{n-q})$$

$$+\sum_{p=2}^{n}\sum_{l_1,l_p=0}^{L} c_{p,0}(l_1,....l_p)H_{n,p}(j\omega_1,...j\omega_n). \tag{31}$$

where the recursive relation is given by

$$H_{n,p}^{asym}(.) = \sum_{i=1}^{n-p+1} H_i(j\omega_1,...j\omega_i)H_{n-i,p-1}(j\omega_{i+1},..j\omega_n)(j\omega_1+...+j\omega_i)^{l_p}. \tag{32}$$

The recursion finishes with $p = 1$ and $H_{n,1}(j\omega_1,....j\omega_n)$ has the property

$$H_{n,1}(j\omega_1,....j\omega_n) = H_n(j\omega_1,...j\omega_n)(j\omega_1+....+j\omega_n)^{l_1}. \tag{33}$$

The above equations for the generalised frequency response function will be used to derive the regression equations for estimating the unknown parameters $c_{p,q}(l_1,..l_{p+q})$ in equation(34).

Note that, the computation of the n-th order frequency response functions is a recursive procedure where each lower order of generalised frequency response function contains no effects from higher order terms. This offers a distinct advantage since the parameters corresponding to different nonlinearities or terms in the continuous time nonlinear differential equation can be estimated one at a time and quite independently ,beginning with first order terms and then building up to include the nonlinear terms.

5.1 Estimation of Linear Terms

The first order frequency response is only related to the linear input-output terms. Setting $n = 1$ in eqn(31) gives

$$-\left[\sum_{l_1=0}^{L} c_{1,0}(l_1)(j\omega_1)^{l_1}\right] H_1(j\omega_1) = \sum_{l_1=0}^{L} c_{0,1}(l_1)(j\omega_1)^{l_1}. \tag{34}$$

Without loss of generality it is assumed that the parameter corresponding to the linear output term $c_{1,0}(0)$ is unity. Moving all other terms to the right hand side gives

$$-H_1(j\omega_1) = \sum_{l_1=1,l_1\neq 0}^{L} c_{1,0}(l_1)(j\omega_1)^{l_1}H_1(j\omega_1) + \sum_{l_1=0}^{L} c_{0,1}(l_1)(j\omega_1)^{l_1}. \tag{35}$$

which is linear in the parameters expression. The parameters $c_{1,0}(.)$ and $c_{0,1}(.)$ can be estimated using the weighted complex orthogonal estimator (Swain and Billings,1995) (described in Appendix-A). For clarity compare eqn(35) with eqn(A.1) to relate the parameters of both equations.

So that from equation(A.1)

$$z(j\omega) = \theta_1 p_1(j\omega) + \theta_2 p_2(j\omega) + ... + \theta_M p_M(j\omega) \tag{36}$$

where $M = 2L + 1$ and

$z(j\omega) = -H_1(j\omega_1)$

$\theta_1 = c_{1,0}(1), \qquad p_1(j\omega) = (j\omega_1)H_1(j\omega_1)$

$\theta_2 = c_{1,0}(2), \qquad p_2(j\omega) = (j\omega_1)^2 H_1(j\omega_1)$

$\vdots$

$\theta_L = c_{1,0}(L), \qquad p_L(j\omega) = (j\omega_1)^L H_1(j\omega_1)$

$\theta_{L+1} = c_{0,1}(0), \qquad p_{L+1}(j\omega) = p_M(j\omega) = (j\omega_1)^0 = 1$

$\theta_{L+2} = c_{0,1}(1), \qquad p_{L+2}(j\omega) = (j\omega_1)$

$\theta_{L+3} = c_{0,1}(2), \qquad p_{L+3}(j\omega) = (j\omega_1)^2$

$\vdots$

$\theta_{2L+1} = c_{0,1}(L), \qquad p_{2L+1}(j\omega) = p_M(j\omega) = (j\omega_1)^L$

The proposed estimation algorithm can now be applied to eqn.(36) to identify the unknown parameters by replacing the frequency response function $H_1(j\omega_1)$ by estimates of this function.

5.2 Estimation of Second Order Nonlinearities

To estimate the parameters associated with second order nonlinear terms, set $n = 2$ in eqn.(31) so that

$$\begin{aligned} -\left[\sum_{l_1=0}^{L} c_{1,0}(l_1)(j\omega_1 + j\omega_2)^{l_1}\right] H_2^{asym}(j\omega_1, j\omega_2) = & \sum_{l_1,l_2=0}^{L} c_{0,2}(l_1,l_2)(j\omega_1)^{l_1}(j\omega_2)^{l_2} \\ & + \sum_{l_1,l_2=0}^{L} c_{1,1}(l_1,l_2)(j\omega_2)^{l_2} H_{1,1}(j\omega_1) \\ & + \sum_{l_1,l_2=0}^{L} c_{2,0}(l_1,l_2) H_{2,2}(j\omega_1, j\omega_2). \end{aligned} \tag{37}$$

By the recursive relation

$$H_{1,1}(j\omega_1) = H_1(j\omega_1)(j\omega_1)^{l_1}. \tag{38}$$

$$H_{2,2}^{asym}(j\omega_1, j\omega_2) = H_1(j\omega_1)H_{1,1}(j\omega_2)(j\omega_1)^{l_2}$$

$$= H_1(j\omega_1)H_1(j\omega_2)(j\omega_2)^{l_1}(j\omega_1)^{l_2}. \tag{39}$$

So that finally a linear regression equation is obtained as

$$\begin{aligned} -\left[\sum_{l_1=0}^{L} c_{1,0}(l_1)(j\omega_1 + j\omega_2)^{l_1}\right] H_2^{asym}(j\omega_1, j\omega_2) &= \sum_{l_1,l_2=0}^{L} c_{0,2}(l_1,l_2)(j\omega_1)^{l_1}(j\omega_2)^{l_2} \\ &+ \sum_{l_1,l_2=0}^{L} c_{1,1}(l_1,l_2)(j\omega_2)^{l_2} H_1(j\omega_1)(j\omega_1)^{l_1} \\ &+ \sum_{l_1,l_2=0}^{L} c_{2,0}(l_1,l_2) H_1(j\omega_1)H_1(j\omega_2)(j\omega_1)^{l_2}(j\omega_2)^{l_1}. \end{aligned} \tag{40}$$

Notice that the parameters $c_{1,0}(l_1), l_1 = 0, ...L$ on the left hand side have been estimated as linear terms initially while all the parameters on the right hand side of the equation can be estimated from eqn(37) by replacing the first and second order frequency response functions by their estimates and applying the estimator.

5.3 Estimation of Higher Order Nonlinearities

When dealing with higher order terms (n=3,4,..),some parameters which have been obtained in previous stages (for orders less than the 'nth') appear on the right hand side of the equation. These are associated with lower order pure output and cross-product terms but not pure input terms.Moving these terms to the left hand side gives

$$\begin{aligned} &- \left[\sum_{l_1=0}^{L} c_{1,0}(l_1)(j\omega_1 + ...j\omega_n)^{l_1}\right] H_n^{asym}(j\omega_1, ...j\omega_n) \\ &- \sum_{q=1}^{n-2}\sum_{p=1}^{n-q-1}\sum_{l_1,l_n=0}^{L} c_{p,q}(l_1, ...l_{p+q})(j\omega_{n-q+1})^{l_{p+1}}...(j\omega_n)^{l_{p+q}} H_{n-q,p}(j\omega_1, ..j\omega_{n-q}) \\ &- \sum_{p=2}^{n-1}\sum_{l_1,l_p=0}^{L} c_{p,0}(l_1, ...l_p) H_{n,p}(j\omega_1, ...j\omega_n) \\ &= \sum_{l_1,l_n=0}^{L} c_{0,n}(l_1, ...l_n)(j\omega_1)^{l_1}...(j\omega_n)^{l_n} \\ &+ \sum_{q=1}^{n-1}\sum_{l_1,l_n=0}^{L} c_{p,q}(l_1, ...l_n)(j\omega_{n-q+1})^{l_{p+1}}..(j\omega_n)^{l_{p+q}} H_{n-q,n-q}(j\omega_1, ..j\omega_{n-q}) \\ &+ \sum_{l_1,l_n=0}^{L} c_{n,0}(l_1, ...l_p) H_{n,n}(j\omega_1, ..j\omega_n). \end{aligned} \tag{41}$$

The reconstruction is achieved by applying the weighted complex orthogonal estimator (Appendix-A). Full details of the algorithm, the properties and guidelines for implementation can be found in Swain and Billings (1995). The weighting matrix 'Q' in all the examples has

been taken to be

$$Q = diag[q_1(\omega), q_2(\omega), ...q_N(\omega)] \tag{42}$$

where '$q_i(\omega)$' is a monotonically decreasing exponential of the form

$$q_i = exp(-\omega_i^2/\lambda) \tag{43}$$

The weighting parameter 'λ' controls the distribution of the weights of the errors for each frequency 'ω'

Examples

In the following sections, wave force data from a variety of systems have been modelled by applying the techniques and procedures described in previous sections. In all the examples the models have been fitted and analysed in the following manner:

- Fit a discrete NARMAX model to the sampled input-output data by applying an orthogonal least squares (OLS) estimator
- Compute and interpret the generalised frequency response functions of the estimated NARMAX model.
- Fit a Morison equation model to the input-output data using conventional least squares curve fitting techniques and make a comparative analysis with respect to the NARMAX model
- Estimate nonlinear continuous time differential equation models by curve fitting to the generalised frequency response functions.

6 Modelling of Small Scale Wave Force Data

The velocity and force time histories for twenty two different rectangular wave spectra with a fixed cylinder were obtained from the University of Salford (Baker,1994). The cylinder was subjected to random waves with rectangular spectral density functions having different bandwidths. The force was measured on a small cylindrical element and the input velocity is the ambient horizontal water particle velocity at the mid point of the element (obtained without the cylinder in position). These data were sampled with an uncertainty of 40μsec. All wave tests had a variance of water surface elevation of $650mm^2$. The flow conditions were described by three parameters : KC,Re and β where KC, the Keulegan-Carpenter number, is defined in the present study as $\frac{\sqrt{(2)}u_{rms}T_w}{D}$, Re is the Reynolds number $\frac{\sqrt{(2)}u_{rms}D}{\nu}$, β is the

Stokes number defined as $\frac{D^2}{T_w \nu}$, u_{rms} is the root mean square (rms) value of the horizontal velocity, T_w is the period associated with the peak in the velocity spectrum and ν is the kinematic viscosity of fluid. The diameter and length of the cylindrical element are 0.038m and 0.05067m. Relevant information about the data sets used in the present study are shown in Table-1. Further details about the experimental set up can be found in Baker(1994).

Table-1 : Experimental Conditions of Salford Cylinder

Tests on Constrained Cylinder	Minimum Frequency Hz	Maximum Frequency Hz	Spectral Bandwidth Hz	Sampling Interval sec	No.of Data Collected	Flow Parameters (KC,β, Re)
Data Set-1	0.3239	0.6002	0.2763	0.02	20972	KC=4.74, β=667.2 Re=3.1638E+03
Data Set-2	0.2570	0.6476	0.3906	0.02	19437	KC=4.95, β=653.11 Re=3.2332E+03
Data Set-3	0.1657	0.7339	0.5682	0.02	16879	KC=4.46, β=649.51 Re=2.9021E+03

6.1 Discrete Time Modelling

Models were fitted between the inline force and the horizontal water particle velocity. The input-output data were decimated by a factor of 2 (effective sampling frequency of 25Hz) using the decimate function available in MATLAB (1992) This function filters the data with an eighth order Chebyshev Filter that is basically a lowpass filter having a cutoff frequency equal to

$$f_{cutoff} = \frac{0.8 * f_s}{2R} \tag{44}$$

where f_s is the sampling frequency of the original data and R is the decimation factor. The original spectral information of the data is not lost due to decimation. The above sampling was chosen using the procedures described in section 3.3. In order to fit a discrete NARMAX model,700 data points were used for estimation purposes and the model validation was done with a sequence of 1000 points of input-output data taken arbitrarily from the rest of the available data points. The discrete NARMAX models were fitted to the data sets-1,2 and 3 with an initial model specification of $n_u = 3$,$n_y = 3$, $n_e = 10$, $N_l = 3$. The terms that were selected together with their associated parameter estimates, error reduction ratios (ERR) and the standard deviation of the parameters are tabulated in Table-2.1,2.2 and 2.3. Note that from no *a priori* knowledge, the estimator selects the significant terms to include in the model and ranks them in the order given in Table-2.1,2.2 and 2.3. Multiplying the ERR values by 100 gives the % contribution that each term makes to the variance of the output.

The estimated noise model is given in the last row of each table. Note that the estimation of noise model is essential to ensure that the parameters of the process model are unbiased.

Table-2.1 : Results of Orthogonal Estimator for Data Set-1

terms	estimates	ERR	$\sigma_{est.}$
y(k- 1)	0.15593E+01	0.98545E+00	0.90788E-01
y(k- 2)	-0.44738E+00	0.13507E-01	0.16114E+00
y(k- 3)	-0.15585E+00	0.60027E-04	0.77194E-01
u(k- 1)	0.12829E+01	0.72154E-05	0.16776E+00
u(k- 3)	-0.11957E+01	0.18119E-03	0.16177E+00
u(k- 3)u(k- 3)u(k- 3)	0.48262E+01	0.38678E-05	0.23974E+01

0.2630 e(k-3)-0.2612e(k-4)-0.239e(k-2)-0.1618e(k-6)-0.0461e(k-7)
+0.0469e(k-9)-0.031e(k-8)+0.025e(k-5)-0.0016e(k-10)+0.00062e(k-1)

Table-2.2 : Results of Orthogonal Estimator for Data Set-2

terms	estimates	ERR	$\sigma_{est.}$
y(k- 1)	0.15459E+01	0.98269E+00	0.81696E-01
y(k- 2)	-0.45829E+00	0.16004E-01	0.14191E+00
y(k- 3)	-0.13742E+00	0.31174E-04	0.67870E-01
u(k- 1)	0.14043E+01	0.21535E-04	0.17364E+00
u(k- 3)	-0.13099E+01	0.21617E-03	0.16841E+00
u(k- 3)u(k- 3)u(k- 3)	0.58851E+01	0.41526E-04	0.12081E+01

-0.2805e(k- 2)-0.171e(k-4)+0.152e(k-3)-0.1186e(k-6)+0.031e(k-7)
+0.067e(k-1)-0.028e(k-8)+0.0128e(k-10)-0.01e(k-5)-0.003e(k-9)

Table-2.3 : Results of Orthogonal Estimator for Data Set-3

terms	estimates	ERR	$\sigma_{est.}$
y(k- 1)	0.10280E+01	0.98606E+00	0.84491E-01
y(k- 4)	-0.43382E+00	0.12405E-01	0.70496E-01
y(k- 2)	0.58203E-01	0.71540E-04	0.12640E+00
y(k- 3)	0.27386E+00	0.29857E-04	0.11942E+00
u(k- 1)	0.18241E+01	0.19159E-04	0.16255E+00
u(k- 3)	-0.17171E+01	0.15014E-03	0.15756E+00
u(k- 3)u(k- 3)u(k- 3)	0.12059E+02	0.42011E-04	0.18696E+01

+0.514e(k-1)-0.138e(k-2)-0.204e(k-6)-0.198e(k-4)+0.148e(k-5)
-0.120e(k-7)-0.099e(k-8)-0.073e(k-9)-0.062e(k-3)+0.042e(k-10)

The correlation plots and model predicted outputs over the estimation and test sets for data set-1 are shown in Figure-1,2 and 3.

The respective plots for the models fitted to other data sets were quite satisfactory and are not given here for space reasons. However, the normalised mean squared errors based on the one step ahead predictions and model predicted outputs are shown in Table-3.

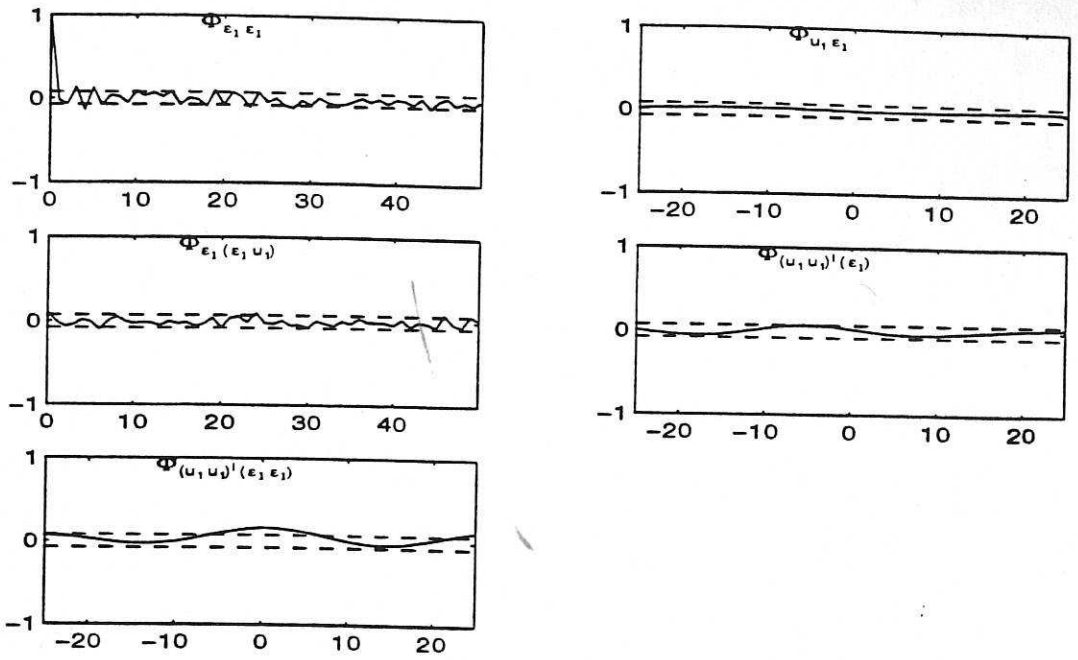

Figure 1: Correlation tests of the NARMAX model of Fixed Cylinder for data set-1

Table-3: Normalised Mean Square Errors of NARMAX models of Salford Cylinder

Model	NMSE of one-step ahead output	NMSE of Model Predicted Output
Data Set-1	0.000656	0.0166
Data Set-2	0.000873	0.0188
Data Set-3	0.00099	0.0228

The results suggest the estimated NARMAX model for data set-1 is unbiased and the predictive performance of the model is excellent. The model generalises well over the rest of the data points, see Fig-1(c), and may be used for predicting the wave forces for any set of input data.

6.2 Frequency Domain Analysis

The plots of the linear and third order frequency response functions of the estimated discrete NARMAX model for data set-1 are shown in Figure-4 a,b,c and d.

The magnitude plot of $H_1(f_1)$ shows a peak value of 20.10db at a frequency 0.825Hz which corresponds to the linear resonant frequency and thereafter decreases monotonically. This is in contrast to the linear frequency response of the general form of the Morison model (eqn(6)) which increases with frequency. Since the NARMAX model of the system does not contain any second order nonlinear term $H_2(f_1, f_2)$ is absent. From the gain plot of the third

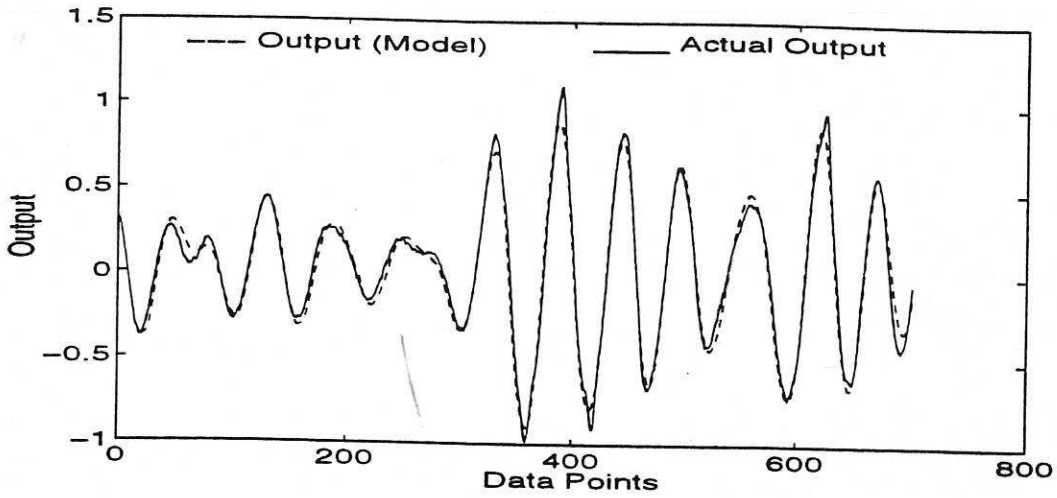

Figure 2: Model Predicted Output of the NARMAX model of Fixed Cylinder for data set-1: Estimation Set

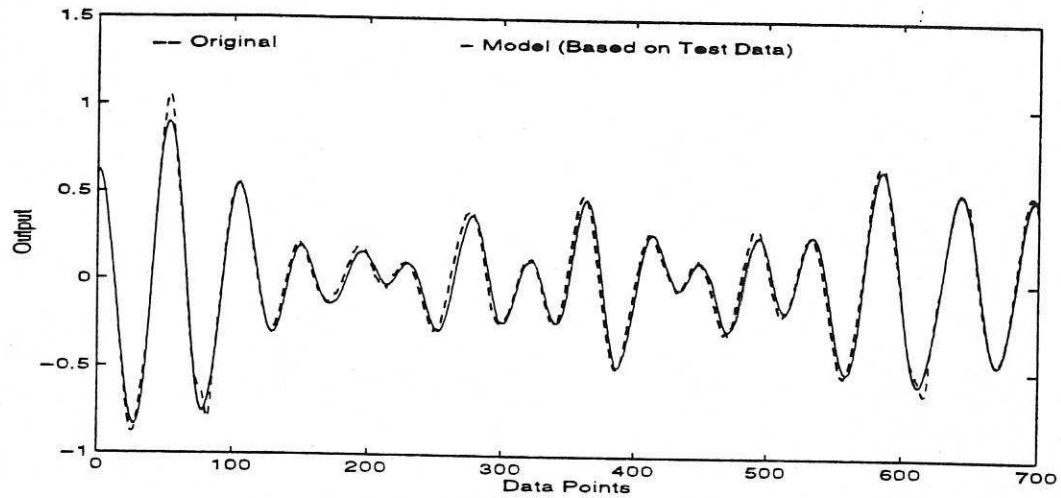

Figure 3: Model Predicted Output of the NARMAX model of Fixed Cylinder for data set-1:Test Set

order frequency response function ,the peak magnitude of $H_3(.)$ is found to be 40.98db. This compares with a maximum of the linear gain of 20.1db and shows that the system possesses a dominant nonlinear characteristic. This occurs when the system is excited by an input whose frequency sum equals 0.55Hz that is when $f_1 + f_2 + f_3 = 0.55$Hz which corresponds to the ridge in the contour plot. This shows that there will a significant amount of energy shift to the lower frequency region under certain conditions of input excitation due to the nonlinear effects. This can not be explained from the Morison model where $H_3(.)$ (eqn(7)) will be a constant for all frequencies with no ridges. The information from the frequency response functions of the estimated models shown in Table-2.2-2.3 is summarised in Table-4 and this shows a reasonable consistency over the data sets which represent excitation at different bandwidths.

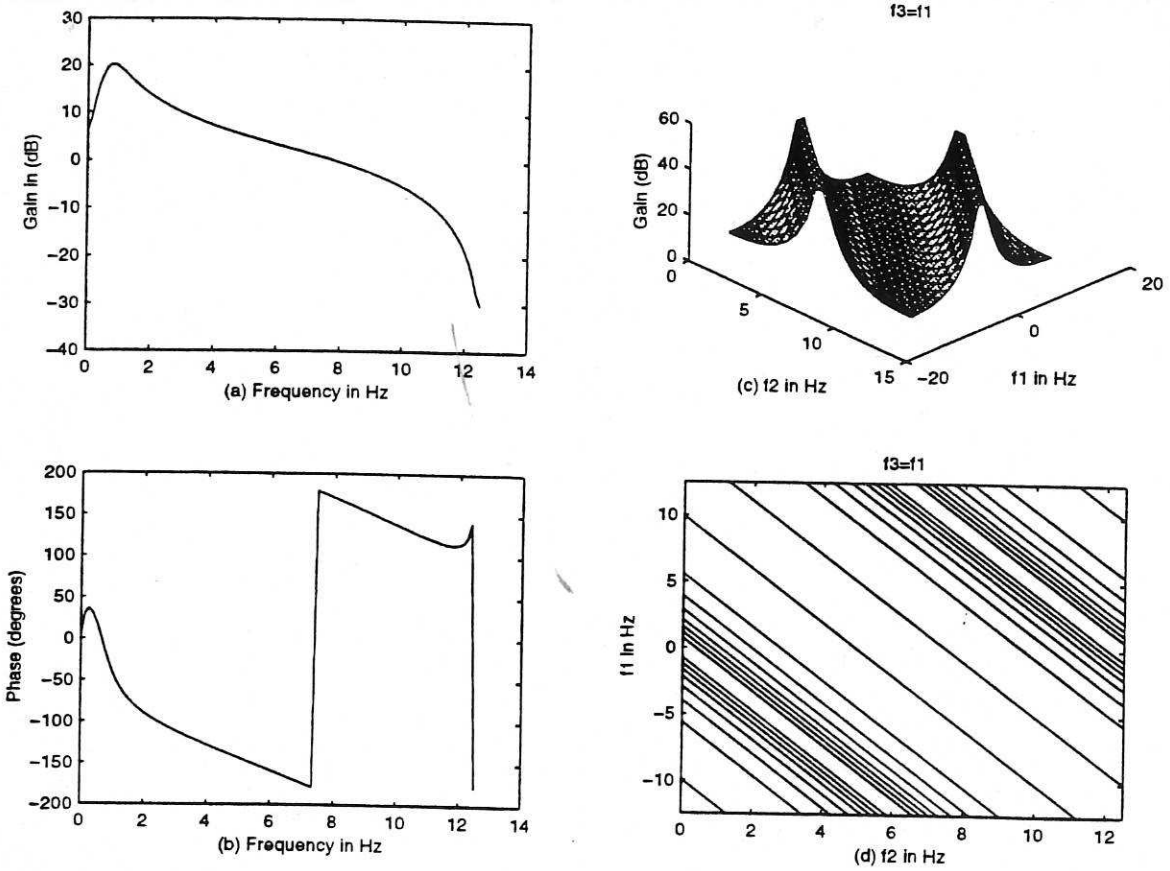

Figure 4: (a) Gain ($H_1(f_1)$ (b).Phase (c) Gain $H_3(f_1, f_2, f_3)$ (d) Gain Contour for the NARMAX model of Data-Set-1

Table-4:Characteristics of the Frequency Response Functions of NARMAX Models of Salford Cylinder

Model	Resonant Frequency (Linear) in Hz	Max.Linear Gain (dB)	Ridge Equation	Max. Nonlinear Gain(dB)
Data Set-1	0.825	20.1014	$f_1 + f_2 + f_3 = 0.55$	40.988
Data Set-2	0.900	20.03	$f_1 + f_2 + f_3 = 0.475$	41.47
Data Set-3	0.775	19.99	$f_1 + f_2 + f_3 = 0.6$	45.92

6.3 Estimation of Nonlinear Continuous Time Models

Having fitted discrete NARMAX models to the input-output data and computing the generalised frequency response functions, the last step of the proposed approach is to estimate continuous time nonlinear differential equation models by curve fitting to the GFRFs. Note that the accuracy of the final estimated continuous time model depends on the accuracy of the discrete model. Hence it will be appropriate to make a comparative analysis of the Morison model with the discrete NARMAX model prior to reconstructing nonlinear continuous time models using the new approach.

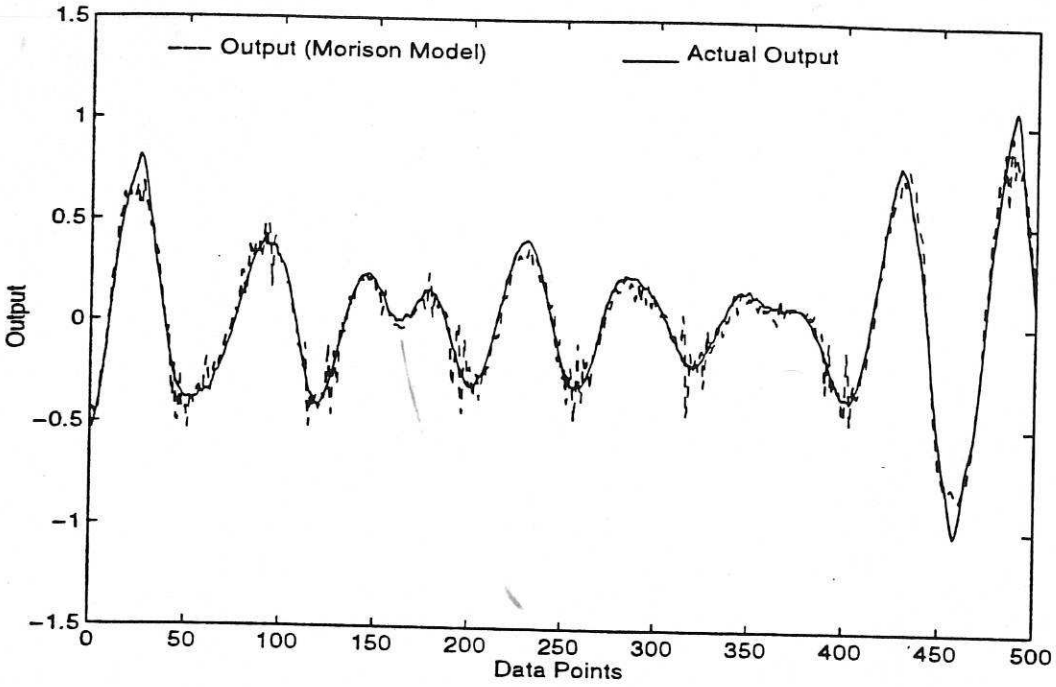

Figure 5: Morison Fit of Data Set-1

6.3.1 Discrete NARMAX vs Morison Model

The Morison equation fitted to the data set-1 using conventional least squares curve fitting is given by

$$y = 2.3264\dot{u} + 34.3064u|u| \tag{45}$$

The approximated Morison equation fitted to the data is given by

$$y = 2.3264\dot{u} + 1.4192u + 175.90u^3 \tag{46}$$

The output of the Morison equation compared with the original output is shown in Figure-5

The Morison equation appears to fit the data quite well. But when estimating the parameters of a given model from a set of input-output data it is essential to investigate whether the model has successfully captured the system dynamics. This is very important if the models are to yield good predictions of the system output for different input excitations and is not simply a curve fit to one data set. It is simple to show that the linear transfer function of the Morison model increases monotonically as the frequency increases thus exhibiting high frequency instability which is not expected from the original input-output data. The Morison models fitted to the other data sets are given in Tables-12-14 and have similar behavior to the present model.

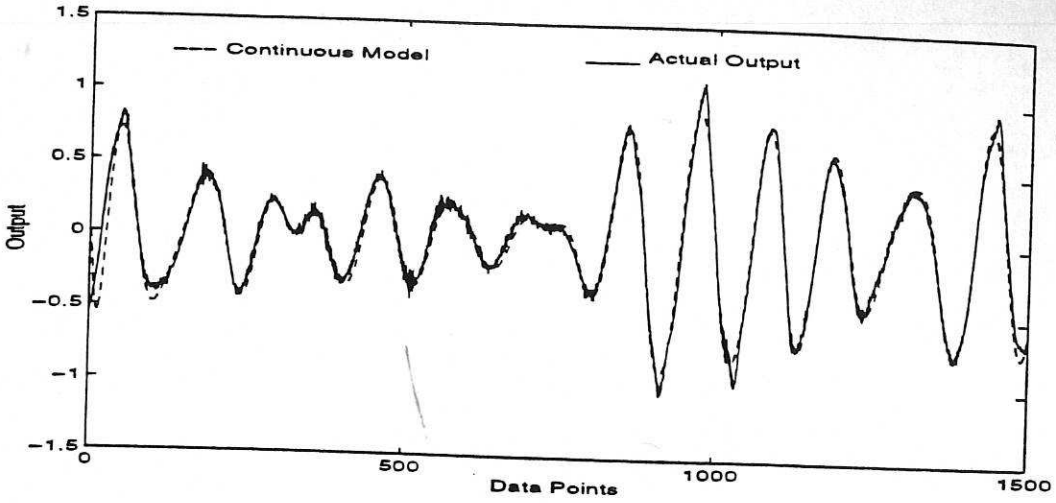

Figure 6: Response of Continuous Time Model for data set-1 of Salford Cylinder

6.3.2 Reconstruction of the Nonlinear Continuous Time Model

It has been shown that the NARMAX model explains the dynamics in the data much better than the Morison model. But the parameters of the NARMAX model can not be easily interpreted. In the present search for a possible extension of the Morison equation, and to have a physically interpretable model, a nonlinear continuous time model needs to be estimated. This is done by curve fitting to the GFRFs computed from the NARMAX model.

The discrete NARMAX model fitted to data set-1 from Table-2.1 is given by

$$\begin{aligned} y(k) &= 1.5593y(k-1) - 0.44738y(k-2) \\ &\quad -0.15585y(k-3) + 1.2829u(k-1) \\ &\quad -1.195u(k-1) + 4.8262u(k-3)u(k-3)u(k-3) \\ &\quad +\Theta_\xi \end{aligned} \tag{47}$$

The last term in eqn.(47) corresponds to the noise terms in Table-2.1.

In order to reconstruct the linear part of the continuous time system, 100 equally spaced frequency response data were generated in the frequency range of 0-5Hz and the weighting parameter'λ' was chosen to be 4.0 For the reconstruction of the nonlinear third order part 64 equally spaced frequency response data were generated in the frequency range of 0-0.2Hz. It was found that with the inclusion of a 'u^3' term the sum of the error reduction ratio (err) values equaled 99.77% which means that this term is adequate to capture almost all of the nonlinear dynamics of the system. The final model was given by

$$0.00145\frac{d^3y}{dt^3} + 0.0463\frac{d^2y}{dt^2} + 0.2609\frac{dy}{dt} + y = 2.2701\frac{du}{dt} + 1.983u + 109.855u^3 \tag{48}$$

To further validate the reconstructed continuous time model the output response of the model in eqn(47) was compared with the original data and this is illustrated in Figure-6.

It is evident from Figure-6 that the estimated continuous time model performs well in predicting the output force. Continuous time models were also reconstructed for the models of Data Sets-2 and 3 under identical conditions. The normalised mean square errors of the reconstructed models were compared with the actual output and the results are summarised in Table-5. The reconstructed models for the other data sets are shown in Tables-13-14.

Table-5:Normalised MSE of Reconstructed Models of Salford Cylinder

Model	Normalised Mean Square Error
Data Set-1	0.0339
Data Set-2	0.0427
Data Set-3	0.0656

7 Modelling of Wave Force Data from a Directional Sea State

In this section the new model structures are fitted to forces and velocities measured on the 0.48m diameter column of the Christchurch Bay Tower described by Bishop(1979). The sea states have wave heights of 7m and are directional with a prominent current. The forces were measured on a section of column 0.535m long and the velocities were measured with calibrated perforated ball meters attached at a distance of 1.228m from the cylinder axis. This will not give the exact velocity at the center of the force sleeve unless waves are unidirectional with crests parallel to the line joining the velocity meter to the cylinder. This is called the Y direction and the normal to this is the X direction. The waves are, however, always varying in direction so in order to facilitate the fitting of a single-input-single-output (SISO) model, the data was chosen from an interval when the oscillatory velocity in the X direction was large and that in the Y direction small. The KC,Re and β values of the data are 20.56, 5.21×10^5 and 2.53×10^4

To fit a discrete NARMAX model all the available 1000 data points were used for estimation. The model was fitted to the input-output data with an initial model specification of $N_l = 3$, $n_u = 2$,$n_y = 3$,$n_e = 20$. The selected terms together with the associated parameter estimates, error reduction ratios and standard deviation of the parameters with proper model validation are shown in Table-6.

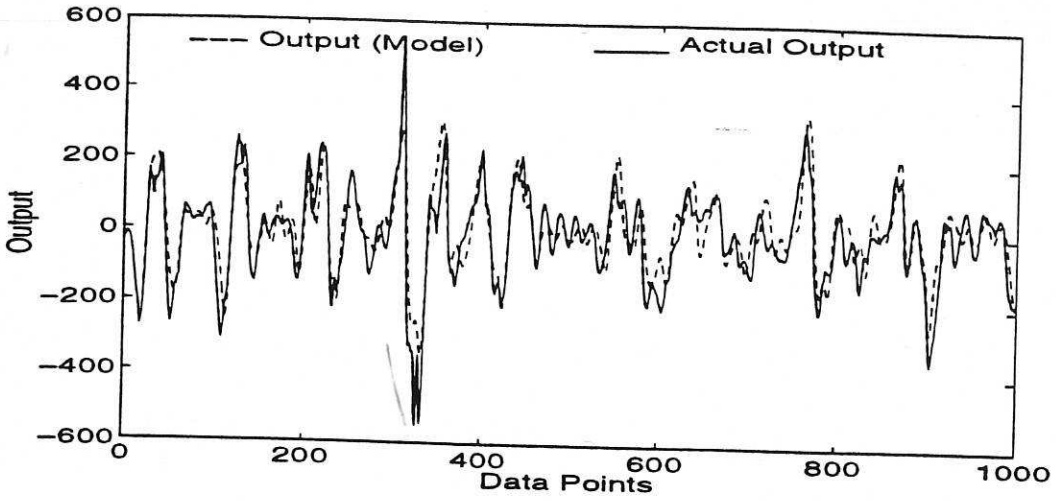

Figure 7: Model Predicted Output of NARMAX model of Christchurch Bay data

Table-6 : Results of Orthogonal Estimation for Chirstchurc Bay Data

terms	estimates	ERR	$\sigma_{est.}$
y(k- 1)	0.23243E+01	0.95596E+00	0.16485E+00
y(k- 2)	-0.19528E+01	0.29568E-01	0.28459E+00
y(k- 3)	0.56292E+00	0.33298E-03	0.13803E+00
u(k- 2)	-0.55953E+02	0.16349E-04	0.14688E+02
u(k- 1)	0.57434E+02	0.14759E-02	0.15304E+02
u(k- 1)u(k- 1)u(k- 1)	0.15184E+01	0.19230E-03	0.71454E+00

+0.1478e(k-6)+0.107e(k-15)-0.0457e(k-3)-0.097e(k-18)
-0.568e(k-1)+0.164e(k-4)+0.054e(k-17)+0.063e(k-20)
+0.0638e(k-5)+0.0505e(k-9)-0.068e(k-16)-0.044e(k-13)
-0.036e(k-7)+0.0395e(k-2)-0.026e(k-12)

The model predicted output is shown in the Figure-7.

The normalised mean square errors based on one step ahead prediction and model predicted outputs are shown in Table-7.

Table-7: Normalised Mean Square Error of NARMAX models of Christchurch Bay

Model	NMSE of one-step ahead output	NMSE of Model Predicted Output
Chirst Church Bay	0.0114	0.2433

From the results it is found that the fitted NARMAX models provided acceptable predictive performance.

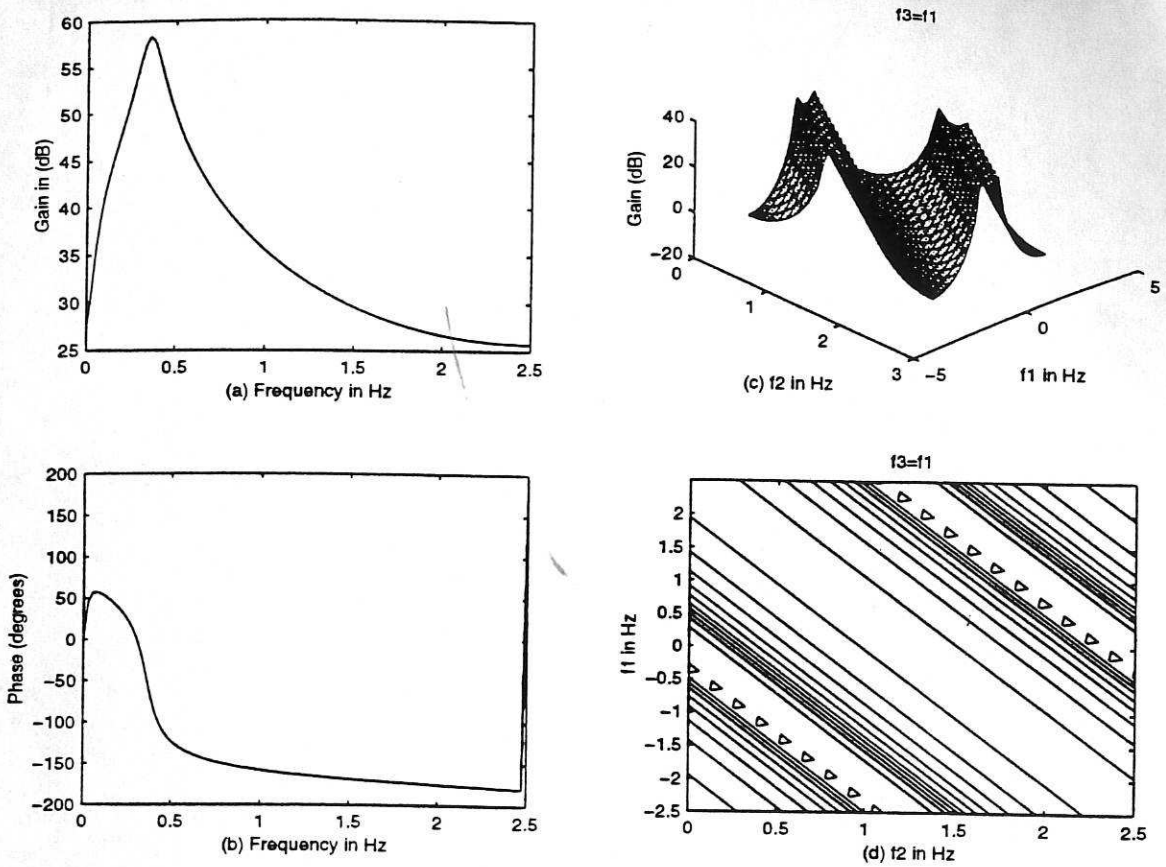

Figure 8: (a) Gain ($H_1(f_1)$ (b).Phase (c) Gain $H_3(f_1, f_2, f_3)$ (d) Gain Contour for the NARMAX model of Christchurch Bay Data

7.1 Frequency Domain Analysis

The gain and phase plots of the linear transfer function and the gain and contour plots for the third order frequency response functions are shown in Fig-8a,b,c and d. The magnitude of the higher order frequency response function shows that there is a significant nonlinear effect.

The plot of the linear frequency response function shows that the linear resonant frequency of the system is 0.3535Hz with a magnitude of 57db and that is followed by a decreasing trend as the frequency is increased. This type of characteristic can not be provided by the Morison model. From the third order frequency response plot, the maximum magnitude of $H_3(.)$ is around 40db indicating that the nonlinear effects of the system are significant. The nonlinear ridges occur due to the interaction among input frequency components whose frequency sum equals 0.375Hz and 0.35Hz.

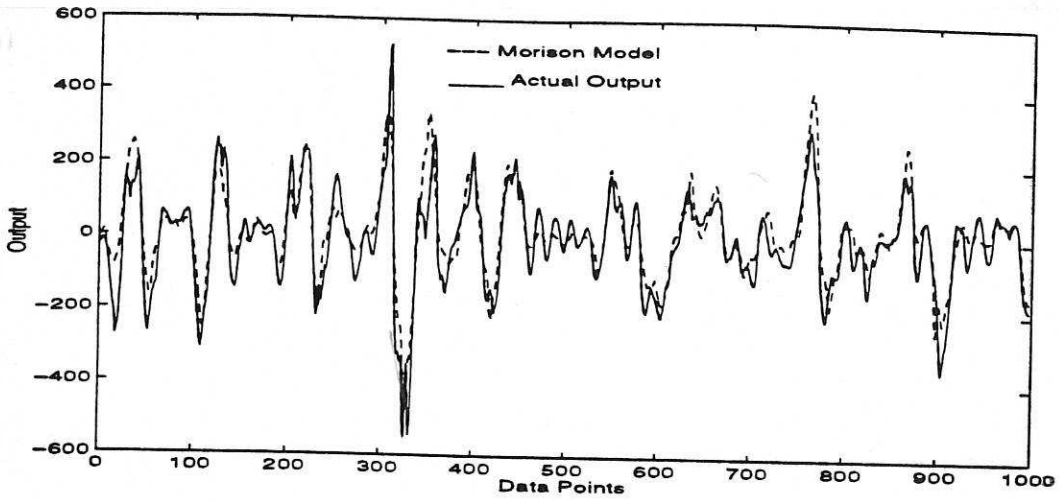

Figure 9: Response of the Morison Model of Christchurch Bay Data

7.2 Estimation of Nonlinear Continuous Time Model of Chirstchurch Bay Model

Morison vs NARMAX

Before estimating the nonlinear continuous time models from the GFRF a Morison equation model was fitted to the data using least squares to yield

$$y(t) = 148.6776\dot{u} + 90.5731u|u| \tag{49}$$

The continuous time Morison equation with cubic approximation of the function $u|u|$ is given by

$$y(t) = 148.6776\dot{u} + 54.339u + 32.02u^3 \tag{50}$$

The response of the Morison equation was compared with the original data and this is shown in Figure-9 which shows a reasonably good fit.

It is simple to show that the Morison model is simply a curve fit to the data and does not correctly represent the underlying dynamics in the data. The third order transfer function $H_3()$ of the Morison model has a magnitude of 30.10db and remains constant at all frequencies and does not posses any ridges compared to the third order transfer function of Figure-8c.

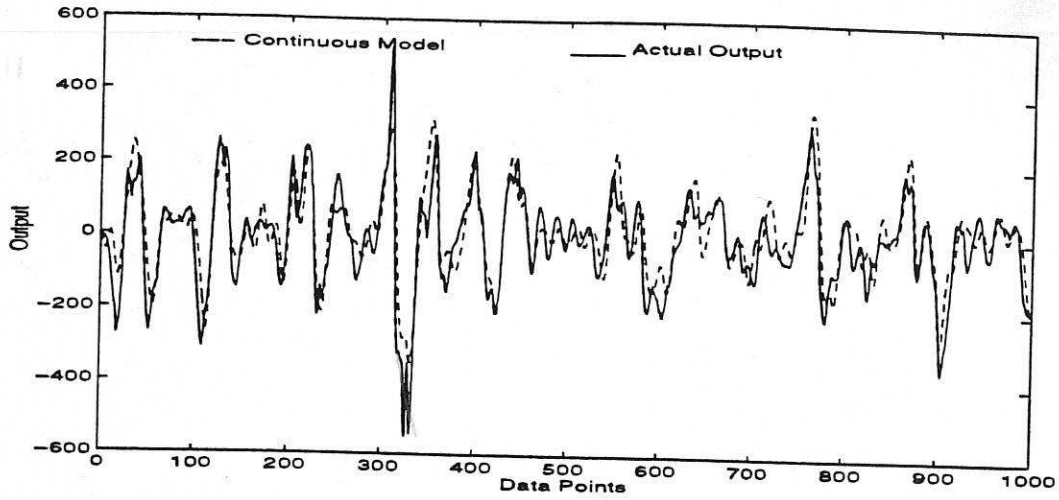

Figure 10: Response of Continuous Time Model of Christchurch Bay Data

7.3 Reconstruction of Continuous Time Models

The discrete NARMAX model of the system is given by

$$\begin{aligned} y(k) &= 2.3243y(k-1) - 1.9528y(k-2) + 0.5629y(k-3) \\ &\quad -55.9534u(k-2) + 57.4343u(k-1) + 1.5184u(k-1)u(k-1)u(k-1) \\ &\quad +\Theta_\xi \end{aligned} \tag{51}$$

In order to reconstruct the linear part of the continuous time system, 100 equally spaced frequency response data were generated in the frequency range of 0-2.5Hz and the weighting parameter 'λ' was fixed at 10. For the reconstruction of the nonlinear part, 64 equally spaced third order frequency response data were generated in the frequency range of 0-0.1Hz. It was found that with the inclusion of the term u^3 the sum of the err values equalled 99.1% which suggests that this term is adequate to capture the nonlinear dynamics of the system. The resulting continuous time model was given by

$$0.089\frac{d^3y}{dt^3} + 0.2581\frac{d^2y}{dt^2} + 0.6101\frac{dy}{dt} + y = 178.69\frac{du}{dt} + 33.6343u + 23.1578u^3 \tag{52}$$

The response of the continuous time model is shown in Figure-10.

The normalised mean square error between the actual output and the output of the reconstructed continuous time system are shown in Table-8.

Table-8: Normalised MSE of Reconstructed Models for Christchurch Bay

Model	Normalised Mean Square Error
Christchurch Bay	0.2562

8 Modelling of Wave Force Data from De Voorst

This data set was obtained from the delta flume of the De Voorst facility at Delft Hydraulics. The particular data considered here comes from run OA1F1 which used a fixed smooth cylinder. The same cylinder was used as in Christchurch Bay but the sea states have smaller wave heights (up to 2m against 7m at Christchurch Bay). The unidirectional wave profiles were generated so that the surface elevation spectrum approximated to a JONSWAP spectrum. More details of the experiment can be found in Davies et al (1990) which contains an exhaustive wave-by-wave Morison analysis of the full De Voorst data set. In the experiment, the horizontal velocity was obtained from electromagnetic flowmeters placed adjacent to the cylinder at the same distance from the wave maker. The forces were recorded from force sleeves placed at three levels (stations 2,3 and 4) on the cylinder. The data from station 2 was discarded as the sleeve fell within the crest to trough region of the wave. Of those remaining,station 3 was nearest to t he surface while fully immersed and was consequently subjected to the highest nonlinear forces. For this reason data from station 3 will be used in the following analysis. The KC,β and Re values of the flow are 5.8030, 4.14×10^4 and 2.40×10^5 respectively.

Out of several thousand input-output pairs of the OA1F1 data set,the most nonlinear data were taken for model estimation. It is known that for the successful identification of any system the input should be persistently exciting so as to excite all the relevant modes (both linear and nonlinear) of the system. In the present example this corresponds to the case where the velocity is high. Since one useful sign of nonlinearity is the size of the transverse component of the force which is caused entirely by vortex shedding, the data for analysis was chosen to be centered about the instant of maximum transverse force excursion.

The model of the De-Voorst tube data was estimated based on the data sampled at 20Hz. In order to fit a discrete NARMAX model, 700 data points were used for estimation and the remaining 300 data points were used for model validation. The model estimated with an initial specification of $N_l = 3$,$n_y = 5$,$n_u = 4$ and $n_e = 20$ with proper model validation is given in Table-9.

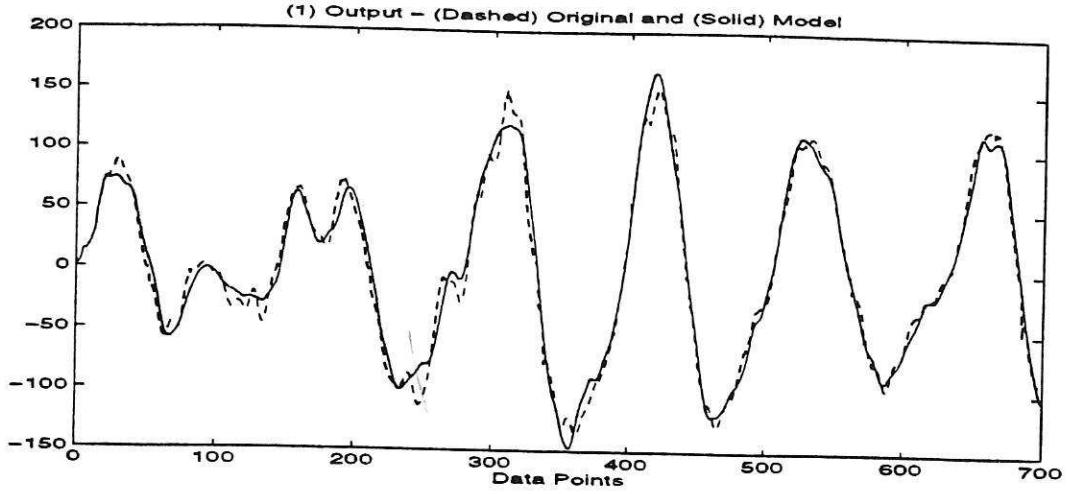

Figure 11: Model Predicted Output of the NARMAX model of the De-Voorst tube:Estimation Set

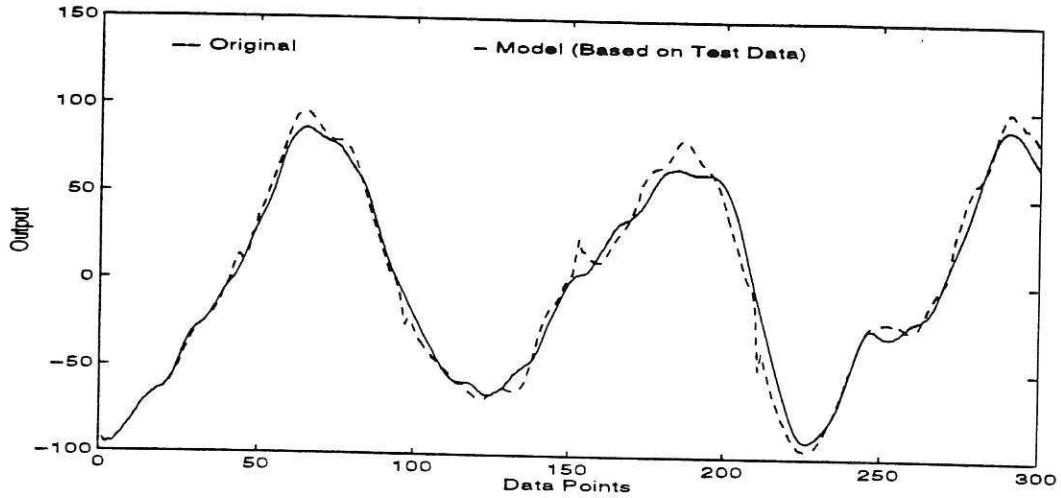

Figure 12: Model Predicted Output of the NARMAX model of De-Voorst tube:Test Set

Table-9: Results of Orthogonal Estimator for De-Voorst Tube

terms	estimates	ERR	$\sigma_{est.}$
y(k- 1)	0.84684E+00	0.99322E+00	0.36790E-01
y(k- 3)	-0.41859E+00	0.31783E-02	0.33035E-01
u(k- 4)	-0.23755E+03	0.28243E-03	0.50806E+02
u(k- 1)	0.29322E+03	0.33148E-03	0.82545E+02
y(k- 2)	0.35113E+00	0.92201E-04	0.49659E-01
u(k- 4)u(k- 4)u(k- 4)	0.16426E+02	0.71055E-04	0.24373E+01
u(k- 2)	-0.57093E+02	0.16406E-04	0.12668E+03

+0.364e(k-3)-0.192e(k-20)+0.179e(k-4)-0.138e(k-17)+0.094e(k-5)
-0.10e(k-18)+0.071e(k-13)+0.0692e(k-9)-0.050e(k-7)

The model predicted output and the model validated outputs are shown in Figure-11 and 12.

The normalised mean square errors based on one step ahead prediction and model pre-

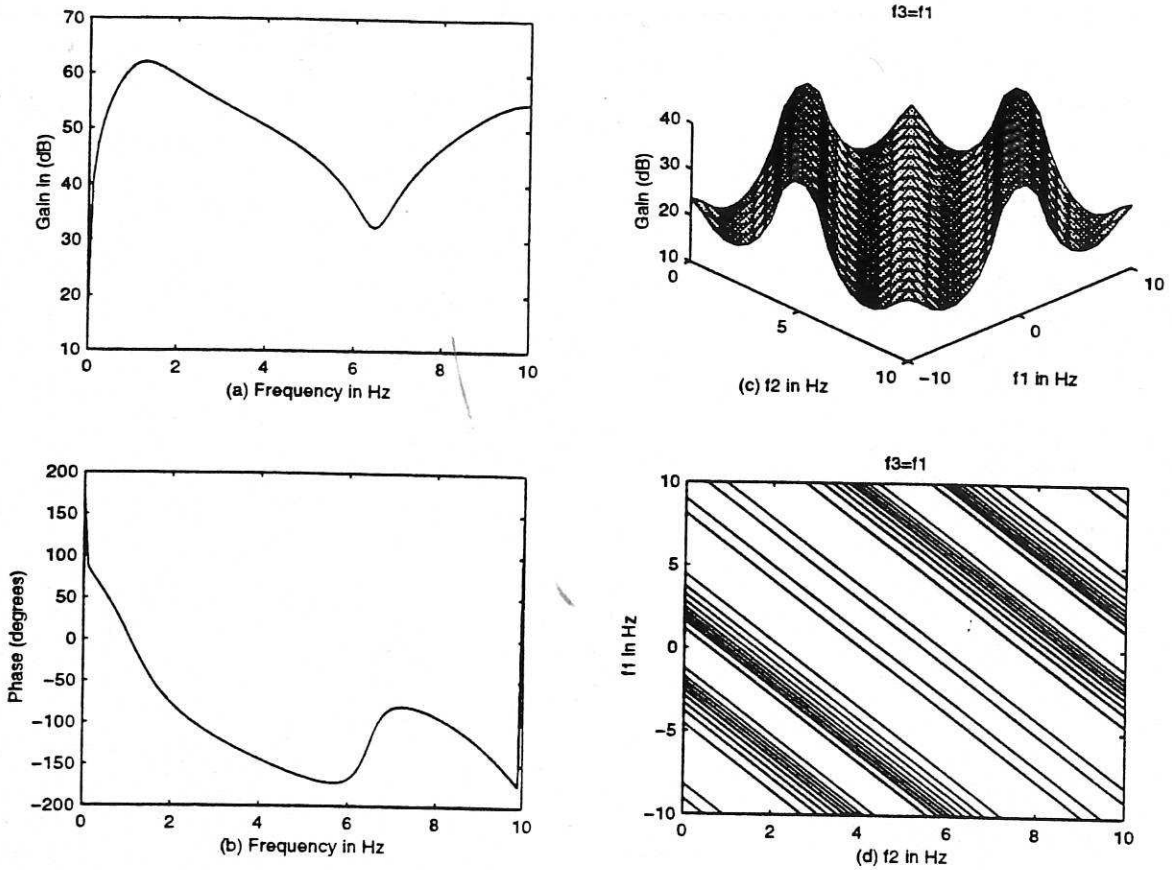

Figure 13: (a) Gain ($H_1(f_1)$ (b).Phase (c) Gain $H_3(f_1, f_2, f_3)$ (d) Gain Contour of De-Voorst Tube model

dicted outputs are shown in Table-10.

Table-10: Normalised Mean Square Error of NARMAX models of De-Voorst Tube Data

Model	NMSE of one-step ahead output	NMSE of Model Predicted Output
De-Voorst Tube	0.0023	0.0192

8.1 Frequency Domain Analysis

The linear and third order frequency response functions of the model in Table-9 are shown in the Figure-13a,b,c and d. From the linear frequency response plots it is evident that the magnitude of $H_1(.)$ reaches a maximum value of around 60db. It does not show a continually increasing trend. The magnitude of the higher order frequency response function shows that there is a significant nonlinear effect represented by the ridges in Figure-13c which occur when the sum of the frequencies of the input excitation equals 0.4Hz.

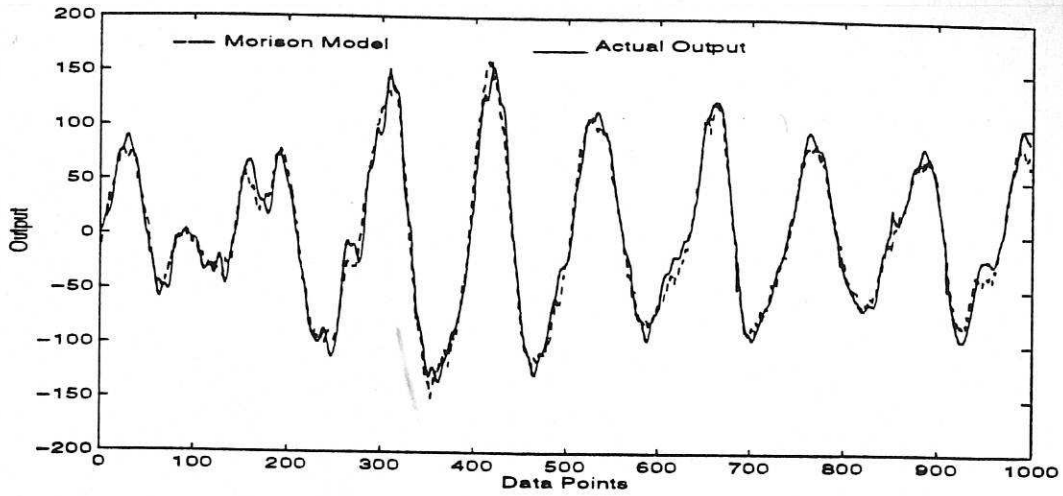

Figure 14: Response of Morison Model of De-Voorst Tube Data

8.2 Estimation of Nonlinear Continuous Time Model

8.3 Discrete NARMAX vs Morison Model

The Morison model estimated from the data by least square was given by

$$y(t) = 169.666\dot{u} + 95.9804u|u| \tag{53}$$

The continuous time Morison equation with cubic approximation of the function $u|u|$ was given by

$$y(t) = 169.666\dot{u} + 27.054u + 72.22u.^3 \tag{54}$$

The response of the Morison equation is compared with the original data in Figure-14

The magnitude of third order transfer function $H_3()$ is 37.17db which remains constant for all frequencies.

8.4 Reconstruction of the Continuous Time Model

From Table-9, the discrete NARMAX model is given by

$$\begin{aligned} y(k) \;=\; & +0.84684y(k-1) - 0.41859y(k-3) \\ & -237.55u(k-4) + 293.22u(k-1) \\ & +16.426u(k-4)u(k-4)u(k-4) - 57.09u(k-2) + \Theta_\xi \end{aligned} \tag{55}$$

The linear part of the continuous time model was reconstructed by generating 100 equally spaced frequency response data in the frequency range 0-2.5Hz and the weighting parameter λ was fixed at 5.0. For the reconstruction of the nonlinear part 64 equally spaced frequency response data in the frequency range 0-0.04 Hz were used. It was found that with the selection

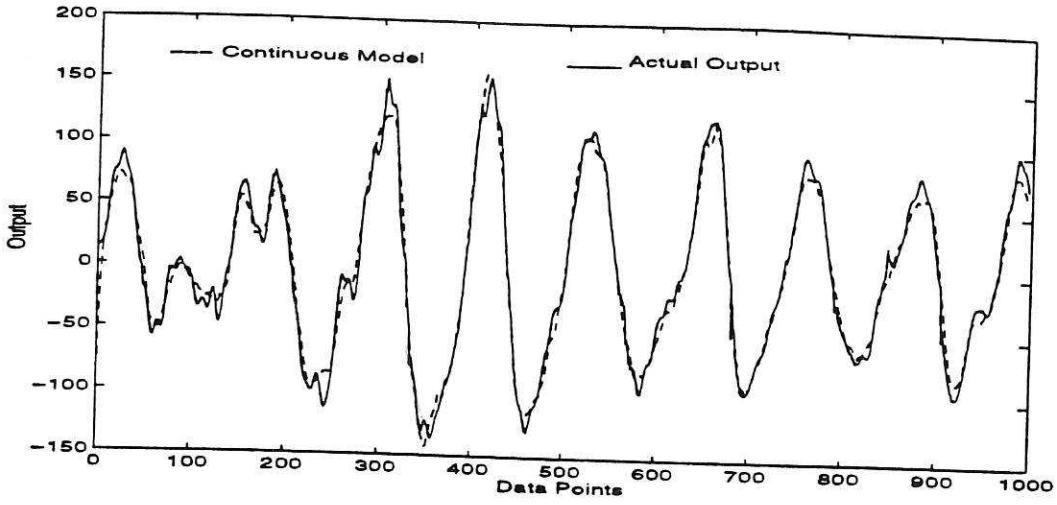

Figure 15: Response of the Continuous Time Model

of the u^3 term the sum of the error reduction ratios became 96% and the contribution of other terms in subsequent iterations was found to be negligible. This implies that the system has a dominant third order nonlinearity in the input. The estimated continuous time model was given by

$$0.02236\frac{d^2y}{dt^2} + 0.1606\frac{dy}{dt} + y = 171.94\frac{du}{dt} + 4.8118u + 74.0056u^3 \qquad (56)$$

The output response of the continuous time model is compared with the original in Figure-15

The normalised mean squared errors between the actual output and the output of the reconstructed continuous time system are given in Table-11.

Table-11: Normalised MSE of Reconstructed Models of De-Voorst Tube Data

Model	Normalised Mean Square Error
De-Voorst Tube	0.0584

9 A Proposed Equation Structure

9.1 Structural Characteristics of Morison's Equation

In the simulated examples based on experimental data it has been observed that the Morison equation fits the data reasonably well but fails to capture the underlying system dynamics. Eqn(4) shows that the Morison equation is essentially an infinite order polynomial in the input with an additional term consisting of the input derivative that partly takes into account the inviscid effect of flow acceleration. The Morison equation is therefore a polynomial approximation to a system and the well known limitations of polynomial curve fitting apply. A polynomial of too low an order cannot capture the structure in the data whereas a polynomial of too high an order will tend to overfit and have poor generalisation properties.

Although the wake flows generating forces in waves are complex phenomena and an accurate representation is often difficult to achieve, it can be shown that the wave force at any particular instant depends on the flow acceleration, the rate of vorticity shed and the flow behavior in the recent past (Stansby,1977). The Morison model can capture the first two effects due to the presence of the input derivative and the drag term but will fail to represent the effects of flow behavior in the past because of the absence of any output dynamics.

An extended version of the Morison equation called the Morison-Duffing equation has been proposed by Stansby et al (1992) to provide a better fit than the Morison equation to data collected from several flow situations. The Morison-Duffing equation is given by

$$\alpha_3\ddot{F} + \alpha_2\dot{F} + \alpha_1 F|F| + F = 0.5\rho D C_d u|u| + 0.25\pi\rho D^2 C_m \dot{u} \tag{57}$$

The higher order derivative terms of the force are included to represent the history effects and the term $F|F|$ has been included to represent other effects of nonlinearity and improve the fit. However, it may be shown that since the drag term $u|u|$ is a polynomial of infinite order, it can emulate all the higher order nonlinear effects which can be represented by the output drag term $F|F|$. Hence the $F|F|$ drag term in the Morison-Duffing equation is not necessary in an equation correctly modelling the dynamic structure which is achieved below.

9.2 Dynamic Morison Equation

The results of fitting nonlinear continuous time differential equation models to data for a variety of flow situations have been given in sections 6-8. Although, in the estimation process, no *a priori* assumptions have been made regarding the structure of the models; both during the estimation of the discrete NARMAX model or during the reconstruction of continuous time models from the higher order frequency response functions, the models obtained in almost all cases show a remarkable consistency. The structure of the continuous time models estimated for the Salford and Christchurch Bay data are of the form

$$\alpha_3\frac{d^3y}{dt^3} + \alpha_2\frac{d^2y}{dt^2} + \alpha_1\frac{dy}{dt} + y = \beta_m\frac{du}{dt} + \beta_{d1}u + \beta_{d3}u^3 \tag{58}$$

and the model for De-Voorst tube has the structure given by

$$\alpha_2\frac{d^2y}{dt^2} + \alpha_1\frac{dy}{dt} + y = \beta_m\frac{du}{dt} + \beta_{d1}u + \beta_{d3}u^3 \tag{59}$$

It has been observed that although perfectly reconstructed continuous time models (sum of ERR equals 100 %) for Salford and Chirstchurch Bay data yield models possessing third order output dynamics, exclusion of the term $\frac{d^3y}{dt^3}$ during the reconstruction phase does not

significantly affect the overall performance of the model. A continuous time model of the form given in eqn(59) seems to be adequate to emulate all the dynamics associated with the wave force data.

The last two terms in the right hand side of the eqn(59) can be assumed to be associated with the drag term. Note that while estimating the NARMAX model it was found that with present available data sets, a third order NARMAX model was sufficient to model all relevant features of the data. Hence the continuous time models estimated possesses nonlinearity up to third degree. However, depending on the different experimental conditions it may not be possible to approximate the system input-output data with a NARMAX model of third order and the corresponding reconstructed nonlinear model may contain higher order nonlinear terms of the input. To accommodate those possibilities a model structure containing an explicit drag term.

$$\alpha_2 \frac{d^2y}{dt^2} + \alpha_1 \frac{dy}{dt} + y = \beta_m \frac{du}{dt} + \beta_d u|u| \tag{60}$$

is preferred. The coefficients β_m and β_d are related to inertia and drag coefficients respectively such that

$$\begin{aligned} \beta_m &= 0.25\pi\rho D^2 C_m \\ \beta_d &= 0.5\pi\rho D C_d \end{aligned} \tag{61}$$

Eqn(60) will therefore be referred to as the **Dynamic Morison** equation.

9.2.1 Characteristics of the Dynamic Morison Equation

- The linear transfer function of the proposed equation is given by

$$H_1(j\omega_1) = \frac{\beta_{d1} + j\omega\beta_m}{1 + j\omega\alpha_2 + (j\omega)^2\alpha_2} \tag{62}$$

  Thus as $\omega \rightarrow \infty$, $H_1(j\omega_1) \rightarrow 0$ implying that it does not suffer from high frequency instability.

- The drag term $u|u|$, in conjunction with the output derivative terms can emulate the nonlinear features of the system to an arbitrary degree of accuracy.

9.3 Parameter Estimation Based on The Dynamic Morison Equation

Having postulating a new model structure eqn(60) the next step is to estimate the parameters $\alpha_1, \alpha_2, \beta_m$ *and* β_d.These can be estimated directly by applying a standard least squares

estimator with noise modelling to the input-output data but this will involve computation of the input and output derivatives. To reduce the effects of noise due to differentiation, the parameters of the approximated form of the new model structure (eqn(59)) were estimated using the reconstruction procedure described in section-6 and the results are shown in the Tables as Dynamic Morison(Reconstructed).

9.4 Summary of Results and Discussion

The results of estimating different forms of continuous time models to all the data sets are summarised in Table-12-16. For each data set the models fitted are

- Morison : Models fitted based on the Morison equation using least squares curve fitting techniques
- Reconstructed (NARMAX) : Continuous time differential equation models reconstructed by curve fitting to the Generalised Frequency Response Functions using the weighted complex orthogonal estimator
- Dynamic Morison (Reconstructed) : Parameters of eqn(59) where the $u|u|$ has been approximated by cubic estimated from the GFRFs.

The predictive performance of these models together with the Dynamic Morison model without history terms have been evaluated based on normalised mean square error. Terms of the form $(\beta_{d1}u + \beta_{d3}u^3)$ in the reconstructed models have been approximated by $\beta_d u|u|$ in a least square sense and the drag coefficients were then calculated using eqn(61).

Table-12 : Continuous Time Models for Data Set-1

	Model	C_m	C_d	NMSE
Morison	$y = 2.3264\frac{du}{dt} + 34.3064\ u\|u\|$	2.05	1.8056	**0.0394**
Reconstructed (NARMAX)	$0.00145\ \frac{d^3y}{dt^3} + 0.0463\ \frac{d^2y}{dt^2} + 0.2609\ \frac{dy}{dt} + y =$ $2.2701\ \frac{du}{dt} + 1.983\ u + 109.855\ u^3$	2.0	1.7573	**0.0339**
Dynamic Morison (Reconstructed)	$0.04564\ \frac{d^2y}{dt^2} + 0.2229\frac{dy}{dt} + y =$ $2.1485\ \frac{du}{dt} + 2.094\ u + 108.1211\ u^3$	1.8936	1.8178	0.0322
Dynamic Morison (Without history term)	$y = 2.1485\ \frac{du}{dt} + 2.094\ u + 108.1211\ u^3$	1.8936	1.8178	0.0621

Table-13 : Continuous Time Models for Data Set-2

	Model	C_m	C_d	NMSE
Morison	$y = 2.1243\frac{du}{dt} + 35.70\ u\|u\|$	1.8715	1.8789	0.0487
Reconstructed (NARMAX)	$0.0012\ \frac{d^3y}{dt^3} + 0.04067\ \frac{d^2y}{dt^2} + 0.2556\ \frac{dy}{dt} + y =$ $2.191\ \frac{du}{dt} + 1.894\ u + 118.113\ u^3$	1.9311	1.7076	0.0427
Dynamic Morison (Reconstructed)	$0.04029\ \frac{d^2y}{dt^2} + 0.22057\frac{dy}{dt} + y =$ $2.086\ \frac{du}{dt} + 1.992\ u + 116.441\ u^3$	1.8385	1.7537	0.0422
Dynamic Morison (Without history term)	$y = 2.086\ \frac{du}{dt} + 1.992\ u + 116.441\ u^3$	1.8385	1.7537	0.0467

Table-14 :Continuous Time Models for Data Set-3

	Model	C_m	C_d	NMS
Morison	$y = 2.1435\frac{du}{dt} + 33.9967\ u\|u\|$	1.8892	1.7893	0.061
Reconstructed (NARMAX)	$0.000484\ \frac{d^3y}{dt^3} + 0.04729\ \frac{d^2y}{dt^2} + 0.2061\ \frac{dy}{dt} + y =$ $1.9302\ \frac{du}{dt} + 1.450\ u + 163.545\ u^3$	1.7012	1.7188	0.065
Dynamic Morison (Reconstructed)	$0.04698\ \frac{d^2y}{dt^2} + 0.19334\frac{dy}{dt} + y =$ $1.9001\ \frac{du}{dt} + 1.4979\ u + 162.322\ u^3$	1.6746	1.7367	0.045
Dynamic Morison (Without history term)	$y = 1.90001\ \frac{du}{dt} + 1.4979\ u + 162.322\ u^3$	1.6746	1.7367	0.072

Table-15 : Summary of Results For Christchurch Bay Data

	Model	C_m	C_d	NMSE
Morison	$y = 148.6776\frac{du}{dt} + 90.5731\ u\|u\|$	1.5351	0.7054	0.2145
Reconstructed (NARMAX)	$0.089\ \frac{d^3y}{dt^3} + 0.2581\ \frac{d^2y}{dt^2} + 0.6101\ \frac{dy}{dt} + y =$ $178.69\ \frac{du}{dt} + 33.6343\ u + 23.1578\ u^3$	1.845	0.4621	0.2562
Dynamic Morison (Reconstructed)	$0.2791\ \frac{d^2y}{dt^2} + 0.563\frac{dy}{dt} + y =$ $171.145\ \frac{du}{dt} + 23.00\ u + 23.25\ u^3$	1.7671	0.4037	0.2596
Dynamic Morison (Without history term)	$y = 171.145\ \frac{du}{dt} + 23.00\ u + 23.25\ u^3$	1.7671	0.4037	0.3084

Table-16 : Summary of Results For De-Voorst Tube Data

	Model	C_m	C_d	NMSE
Morison	$y = 169.666\frac{du}{dt} + 95.9804\ u\|u\|$	1.7518	0.7475	0.0233
Dynamic Morison (Reconstructed)	$0.02236\ \frac{d^2y}{dt^2} + 0.1606\ \frac{dy}{dt} + y =$ $171.94\ \frac{du}{dt} + 4.8118\ u + 74.0056\ u^3$	1.7753	0.4120	0.0584
Dynamic Morison (Without history term)	$y = 171.94\ \frac{du}{dt} + 4.8118\ u + 74.0056\ u^3$	1.7753	0.4120	0.0404

The Dynamic Morison equation(60) has two additional terms with coefficients which may be non-dimensionalised with reference to a time scale. For this purpose the wave period associated with the peak in the spectrum (or the mid point in the case of the Salford data) were chosen. Eqn(60) is thus given by

$$\gamma_2 T_w^2 \ddot{y} + \gamma_1 T_w \dot{y} + y = \beta_m \dot{u} + \beta_d u|u| \tag{63}$$

It is always desirable that coefficients of the equation should vary as little as possible from one situation to another and after experimenting algebraically eqn(63) is written in the form

$$\gamma_0 (\gamma_1 T_w)^2 \ddot{y} + \gamma_1 T_w \dot{y} + y = \beta_m \dot{u} + \beta_d u|u| \tag{64}$$

The results for the five test situations (together with T_w,C_d, C_m, KC,Re values) are given in Table-17. The values of γ_0 are very similar apart from Salford data set-3 which is unusual in that it has a wide band spectrum. The narrower bandwidths for Salford Data Sets-1 and 2 and for the Christchurch Bay and De-Voorst data have $\gamma_0 = 0.86 \pm 0.04$. This is a remarkably small variation considering the range of KC,Re and wave conditions (from unidirectional wave flumes to directional field conditions). It is also interesting to compare the coefficients for the Salford data with those for the De-Voorst flume. The KC values are similar (about 5) but the Reynolds numbers differ in magnitude by approximately a factor of 80. It is generally accepted that vortex shedding becomes weaker as Reynolds number increases (for a comprehensive review of such matters see Sarpkaya and Isaacson,(1981) and Stansby and Isaacson (1987)). Vortex shedding generates the history effects and consistently the value of $\gamma_1 \simeq 0.1$ for the Salford data ($Re \simeq 3 \times 10^3$) and $\gamma_1 \simeq 0.03$ for the De-Voorst data ($Re \simeq 2 \times 10^5$) . On the other hand the Reynolds number of the De-Voorst and Christchurch Bay data are similar (within a factor of 2) but the KC values are very different. At $KC = 6$ for the former vortex shedding is generally less strong than for $KC \simeq 20$ for the latter. The corresponding values of γ_1 are 0.03 and 0.06. The values of γ_1 are therefore consistent with our knowledge of vortex shedding and its dependence on KC and Re.

It is also interesting to note the values of C_d and C_m. C_m varies little but $C_d \simeq 0.4$ at high Reynolds numbers is much smaller than at the lower Reynolds numbers where $C_d \simeq 1.8$

. While this overall trend with Reynolds number is expected, $C_d \simeq 0.4$ is less than what is normally obtained at $Re > 10^5$ from the Morison equation where $C_d \simeq 0.6$.

The results in terms of non-dimensional coefficients are thus quite encouraging but many more situations need to be analysed to confirm these preliminary findings.

Table-17 : Summary of Results

Model	T_w	γ_0	γ_1	C_m	C_d	KC	Re
Data Set-1	2.164	0.90	0.103	1.89	1.82	4.74	3.16×10^3
Data Set-2	2.2109	0.83	0.0997	1.84	1.75	4.95	3.23×10^3
Data Set-3	2.2232	1.26	0.0869	1.67	1.74	4.46	2.90×10^3
Christchurch Bay	9.090	0.88	0.062	1.77	0.40	20.5	5.21×10^5
De-Voorst Tube	5.5555	0.87	0.0289	1.77	0.41	5.80	2.4×10^5

10 Conclusions

Nonlinear continuous time models have been estimated for the wave forces on fixed cylinders from a variety of flow situations using a new procedure that does not involve direct differentiation of the input-output data and performs reasonably well in all the cases. It was shown that while the Morison equation can fit to the data, it generally fails to capture the underlying dynamics of the system. Although the experimental conditions for the data used in the current modelling vary considerably and no *a priori* assumptions were made regarding the structure of either the discrete NARMAX or the nonlinear continuous time models during the estimation phase, the models estimated from all the data sets and the associated frequency response functions show a remarkable consistency. This suggests that there is a consistent underlying model form and a new equation called the Dynamic Morison equation has been proposed. The new equation structure has thus been formulated from a thorough mathematical analysis, experi mental observation and intuitive reasoning to produce an effective model which emulates all the nonlinear and dynamic features of wave force mechanisms and performs well in the prediction of wave forces. This new equation involves two non-dimensional coefficients describing history effects (one of which is almost constant) in addition to the drag and inertia coefficients of the standard Morison equation. These coefficients are consistent with the physical understanding of vortex shedding for widely different Keulegan-Carpenter numbers and Reynolds numbers.

Acknowledgments

AKS gratefully acknowledges the financial support provided by the Commonwealth Scholarship Commission of the United Kingdom and is thankful to Board of Governors, Regional

Engineering College, Rourkela, India for granting study leave. SAB gratefully acknowledges that part of this work was supported by EPSRC.

References

[1] Baker,M (1994), "Wave loading on a small diameter flexibly mounted cylinder in random waves", Ph.D dissertation, University of Salford.

[2] Bendant,J.S. (1990), "Nonlinear System Analysis and Identification from Random Data", John Wiely and Sons

[3] Billings,S.A. (1980), "Identification of Nonlinear Systems- a Survey",Proc. IEE, Pt.D, 127, pp.272-285.

[4] Billings,S.A,and Leontaritis,I.J. (1982),"Parameter Estimation Techniques for Nonlinear systems",Proc. 6th IFAC Symp. on Identification and System Parameter Estimation,Wasington D.C.,pp.505-510.

[5] Billings,S.A. and Voon,W.S.F. (1986),"Correlation based model validity tests for nonlinear models",Int.J.Control,vol.44,pp.235-244.

[6] Billings,S.A.,Korenberg,M.J. and Chen,S (1988),"Identification of nonlinear output affine systems using an orthogonal least square algorithm",Int.J. System Science,Vol.19,pp.1559-1568

[7] Billings,S.A. and Peyton Jones,J.C.(1990)."Mapping Nonlinear Integro-Differential Equations into the Frequency Domain',Int.J.Control, vol.52(4), pp.863-879.

[8] Billings,S.A. and Tsang,K.M. (1989), "Spectral Analysis for Nonlinear Systems, Part-I-Parametric Nonlinear Spectral Analysis, "J. Mech Systems and Signal Processing, vol.3, no.4, pp.319-339.

[9] Billings,S.A. and Zhu,Q. (1994), "Structure Detection for nonlinear dynamic rational models "Int. J. of Control, vol.59 no.6, pp.1439-1463.

[10] Billings,S.A. and Aguirre,L.A. (1994), "Effects of Sampling Time on the Dynamics and Identification of Nonlinear Models",(Submitted for publication)

[11] Bishop,J.R.(1979), "Aspects of large scale wave force experiments and some early results from Christchurch Bay ", National Maritime Institute Report No. NMI R57.

[12] Chakrabarti,S.K.(1987), "Hydrodynamics of Offshore Structures" ,Southampton: Computational Mechanics Publications, Springer Verlag.

3] Davies,M.J.S.,Graham,J.M.R. and Bearman,P.W.(1990), "In-line forces on fixed cylinders in regular and random waves", In Enviornmental Forces on Offshore Structures and their prediction, pp. 113-136, Kluwer Academic Press.

4] Iserman,R. (1980), "Practical Aspects of Process Identification", Automatica.

5] Kim,K.I. and Powers,E.J. (1988),"A digital method of modelling quadratically nonlinear systems with a general random input", IEEE Transactions ASSP, Vol.36, pp.1758-1769.

6] Leontaritis,I.J. and Billings,S.A. (1985), "Input-Output parametric models for Nonlinear Systems,Part-I-Deterministic Nonlinear Systems, Part-II-Stochastic Nonlinear Systems,Int.J.Control,vol.41, pp.303-344.

7] Ljung,L (1987), "System Identification-Theory for the User", Prentice Hall,Inc, Englewood Cliffs, New Jersey.

8] MATLAB (1992), "MATLAB High Performance Numeric Computation and Visualization Software : Reference Guide", The MATH WORKS Inc.

9] Morison,J.R.,O'Brien,M.P, Johnson.J.W. and Schaf.S.A. (1950) "The force exerted by surface waves on piles ", Petroleum Transactions, 189, pp.189-202.

0] Palm,G. and Poggio,T. (1977) "The Volterrs representation and the Wiener expansion: validity and pitfall ", SIAM J. on Applied Mathematics, 33, pt-2

1] Peyton Jones,J.C. and Billings,S.A.(1989), "A recursive Algorithm for computing the frequency response of a class of Nonlinear Difference Equation Models",Int.J.Control,vol.50, no.5,pp.1925-1940.

2] Sarpkaya,T. and Isaacson,M. (1981), "Mechanics of Wave Forces on offshore Structures", Van Nostrand Reinhold Co.

3] Soderstrom,T. and Stoica,P (1989), "System Identification" , Prentice Hall,London.

4] Stansby,P.(1977), "An inviscid model of vortex shedding from a circular cylinder in steady and oscillatory flows", Proc. Civil Engineers, Part-2, Vol-63, pp-865-880.

5] Stansby,P. and Isaacson,M(1987), "Recent developments in offshore hydrodynamics, a workshop report",Applied Ocean Research, Vol-9, pp.118-127.

6] Stansby,P.,Worden,K.,Billings,S.A.,and Tomlinson,G.R.(1992), "Improved Wave Force Classification Using System Identification",Applied Ocean Research,14,pp.107-118.

[27] Swain,A.K. and Billings,S.A.(1995), "Weighted Complex Orthogonal Estimator for Identifying Linear and Nonlinear Continuous Time Models from Generalised Frequency Response Functions",(Submitted for publication).

[28] Unbehauen,H. and Rao,G.P.(1987), "Identification of Continuous Systems",System and Control Series,Amsterdam, North Holland.

[29] Weigend,S.A. and Gershenfeld,N.A. (1993), "Time Series Prediction : Forecasting the Future and Understanding the Past, Proc. of the NATO Advanced Research Workshop on Comparative Time Series Analysis held in Sante Fe, SFI studies in Sciences of Complexity", Proc. vol.XV, Addison-Wesley.

[30] Worden,K.,Stansby,P.K.,Tomlinson,G.R.and Billings,S.A.(1994), "Identification of Nonlinear Wave Forces", J. Fluids and Structures, vol.8, pp.19-71.

A APPENDIX

A.1 Weighted Orthogonal Least Squares

Consider a system which can be modeled as

$$z(j\omega) = \sum_{i=1}^{M} \theta_i p_i(j\omega) + \xi(j\omega) \tag{A.1}$$

where $\theta_i, i = 1, ...M$ are the real unknown deterministic parameters of the system associated with the complex regressors $p_i(j\omega), i = 1, ...M$. $z(j\omega)$ is a complex dependent variable or the term to regress upon and $\xi(j\omega)$ represents the modeling error. Before any attempt is made to estimate the parameters 'θ', the complex variables involved in eqn(A.1) should be partitioned in to real and imaginary parts; otherwise θ could be complex. If 'N' measurements of $z(j\omega)$ and $p_i(j\omega)$ are available at $\omega_i, i = 1, ...N$ the complex system of equation(A.1) can be represented after partitioning in matrix form as

$$Z = P\theta + \Xi \tag{A.2}$$

The weighted complex orthogonal estimator (Swain and Billings,1995) transforms eqn(A.2) in to an auxiliary equation

$$Z = Wg + \Xi \tag{A.3}$$

The properties of the matrix W are such that W^TQW is orthogonal; where 'Q' is a positive definite weighting matrix. Further let

$$V = W^TQ \tag{A.4}$$

The regressors of the auxiliary model of eqn.(A.3) can be obtained recursively from

$$\begin{aligned} w_1(\omega) &= p_1(\omega) \\ w_i(\omega) &= p_i(\omega) - \sum_{k=1}^{i-1} \alpha_{ki} w_k(\omega) \quad for\ k < i \end{aligned} \tag{A.5}$$

where

$$\begin{aligned} \alpha_{ki} &= \frac{\langle (w_k^T(\omega)Q), p_i(\omega) \rangle}{\langle (w_k^T(\omega)Q), w_k(\omega) \rangle} \\ &= \frac{\langle v_k(\omega), p_i(\omega) \rangle}{\langle v_k(\omega), w_k(\omega) \rangle} \quad for\ \ k = 1.....i-1 \end{aligned} \tag{A.6}$$

and ' $\langle .,. \rangle$ ' denotes the dot product of the vectors. The estimates of the i-th element of the auxiliary parameter vector 'g' is given by

$$\hat{g}_i = \frac{\langle Z(\omega), v_i(\omega) \rangle}{\langle v_i(\omega), w_i(\omega) \rangle} \quad for\ i = 1, ...M \tag{A.7}$$

Once the parameters $g_i, i = 1, ...M$ are estimated,the original system parameters $\theta_i, i = 1, ...M$ can easily be recovered according to the formula

$$\hat{\theta} = \hat{g} - (T - I)\hat{\theta} \tag{A.8}$$

that is

$$\begin{aligned} \hat{\theta}_M &= \hat{g}_M \\ \hat{\theta}_k &= \hat{g}_k - \sum_{i=k+1}^{M} \alpha_{ki} \hat{\theta}_i, \quad for\ k = 1, ...M-1 \end{aligned} \tag{A.9}$$

Therefore by using the above equations,the unknown parameters $\theta_i, i = 1, ...M$ can be estimated step by step. The structure of the system or which term to include in the model can be determined by using the error reduction ratio test

$$ERR_i = \frac{g_i^2 \langle v_i(\omega), w_i(\omega) \rangle}{\langle (z^T(\omega)Q), z(\omega) \rangle} \times 100\%, \quad i = 1, ...M \tag{A.10}$$

which gives the percentage contribution that each term makes to the output variance (energy). The value of ERR indicates the significance of a candidate term. Normally at the beginning all available candidate terms are examined and the term which contributes the maximum ERR is included in the model. This is repeated until all candidate terms have been exhausted or the sum of the ERR reaches around 100%.